Transverse Spin Physics At STAR

The Past and Future

Len K. Eun
For The STAR Collaboration
RHIC Users Meeting, Jun 2010

PENNSTATE

Transverse Single Spin Asymmetry

Large Transverse Single Spin Asymmetry(SSA) in forward meson production persists up to RHIC energy.

PRL 92, 171801 (2004)

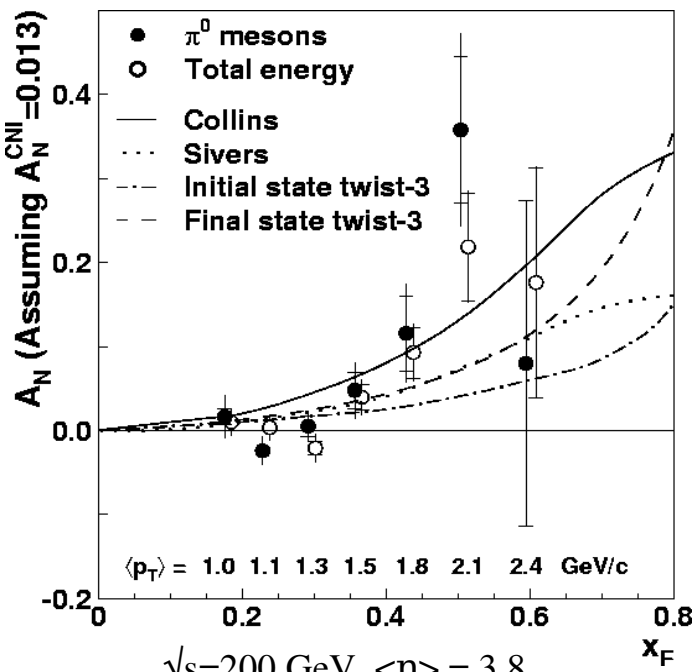

$\sqrt{s}$=200 GeV, $\langle\eta\rangle$ = 3.8

- **Collins effect**: asymmetry comes from the transversity and the spin dependence of jet fragmentation.

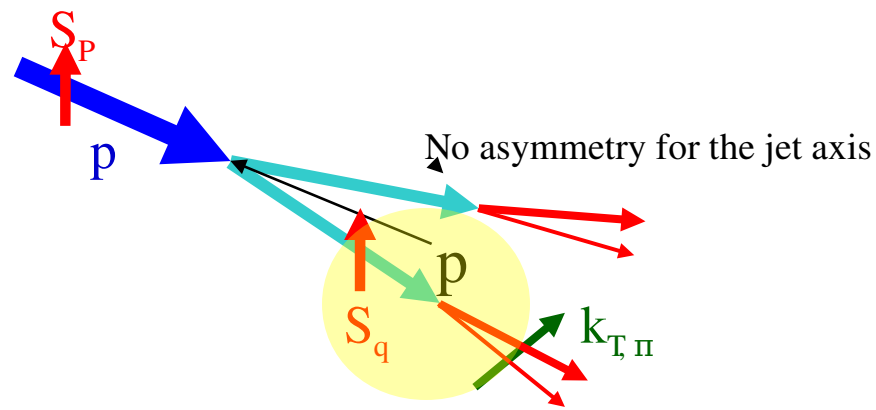

- **Sivers effect**: asymmetry comes from spin-correlated k_T in the initial parton distribution

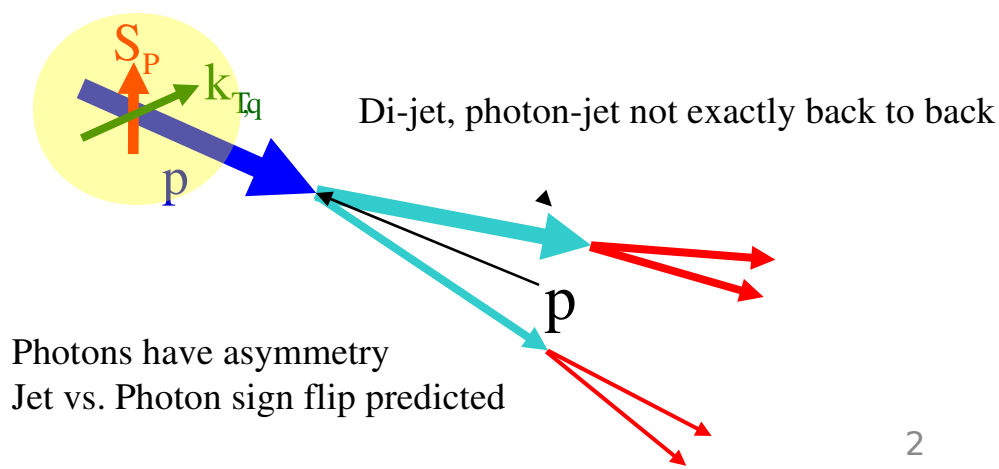

STAR Forward Pion Detector (FPD)

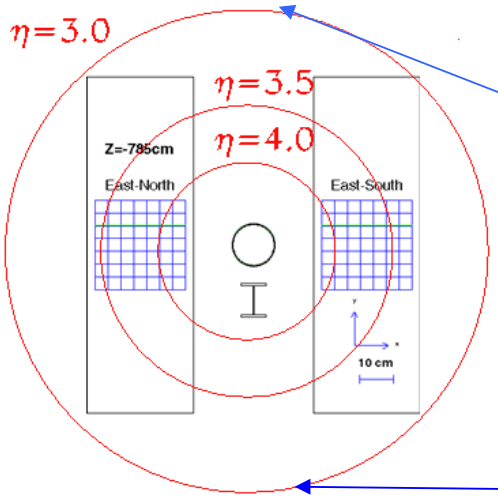

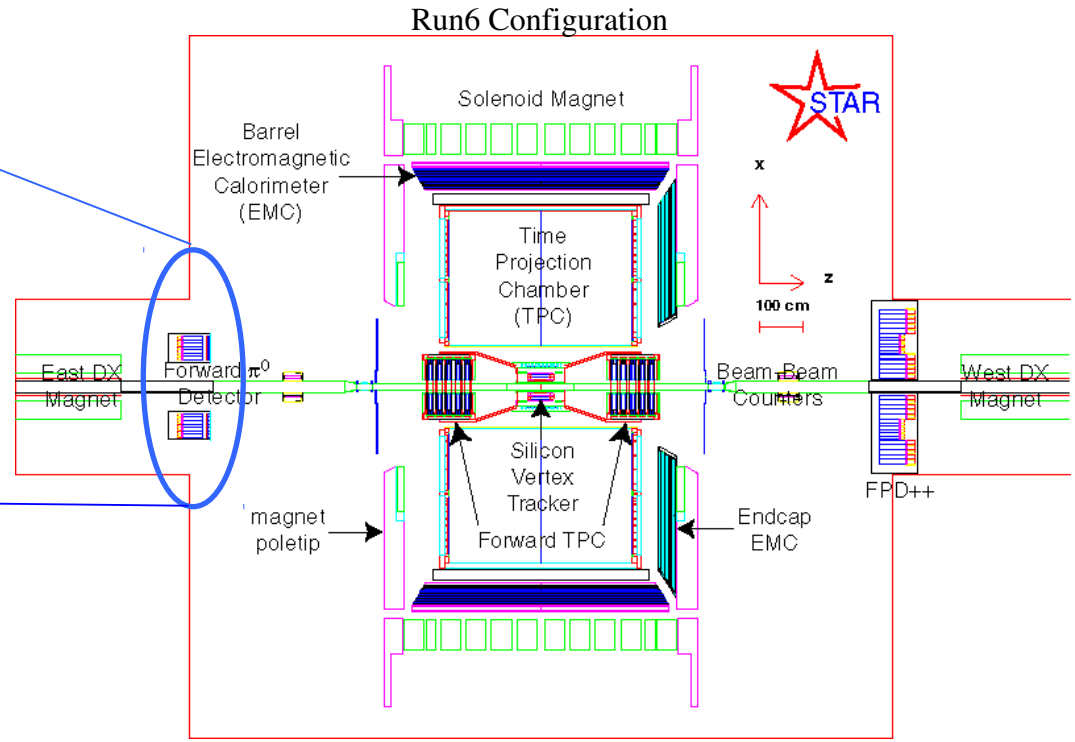

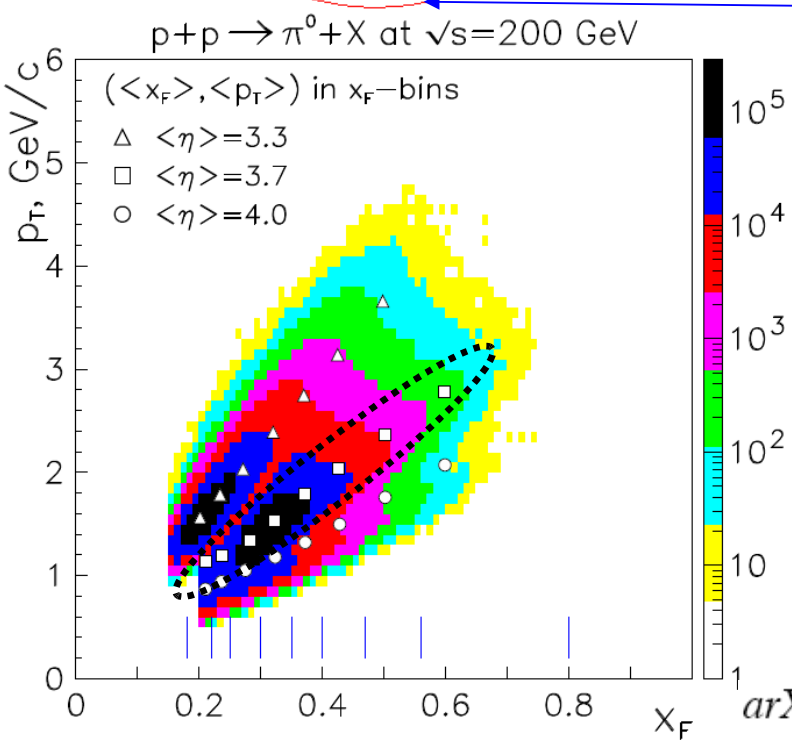

- STAR forward calorimeters have gone through significant upgrades since run3.
- In run6, the original FPD remained in the east, while the west FPD was expanded to FPD^{++}.
- The east FPD consists of two 7X7 Pb-glass modules, EN and ES. During run6, it was placed at the "far" position. (x-offset~30cm, <η>~3.7)

arXiv:0801.2990v1 [hep-ex]

Forward π^0 Single Spin Asymmetry(SSA)

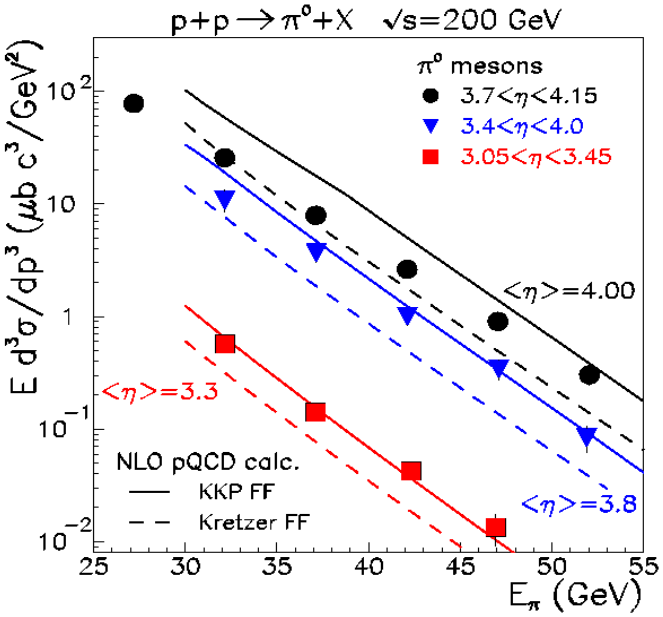

Phys. Rev. Lett. 97 (2006) 152302

At √s=200GeV, π^0 cross-section measured by STAR FPD is consistent with the NLO pQCD calculation. Results at <η>=3.3 and <η>=3.8 have been included in the DSS global pion fragmentation function analysis. *(Phys.Rev.D75(2007) 114010)*

$$A_N = \frac{d\sigma_\uparrow - d\sigma_\downarrow}{d\sigma_\uparrow + d\sigma_\downarrow} \simeq \frac{1}{P}\frac{\sqrt{N_\uparrow S_\downarrow} - \sqrt{N_\downarrow S_\uparrow}}{\sqrt{N_\uparrow S_\downarrow} + \sqrt{N_\downarrow S_\uparrow}}$$

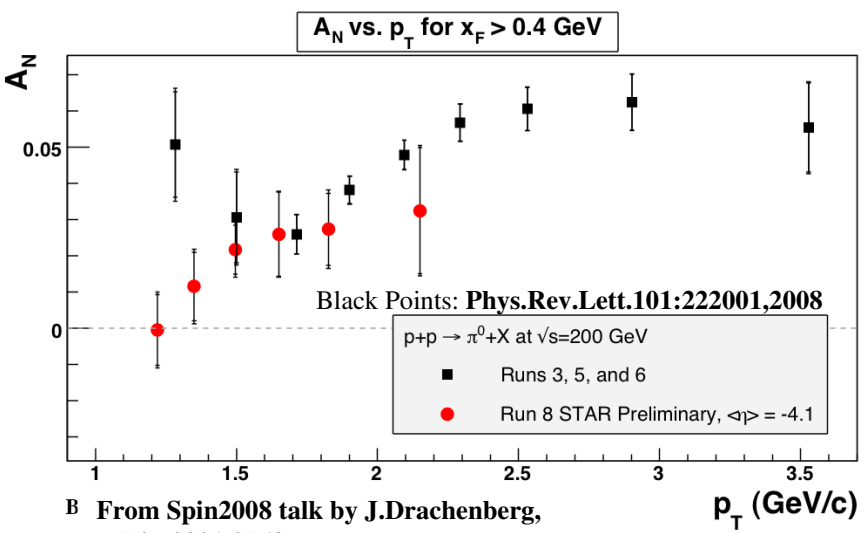

B From Spin2008 talk by J.Drachenberg, arXiv:0901.2763

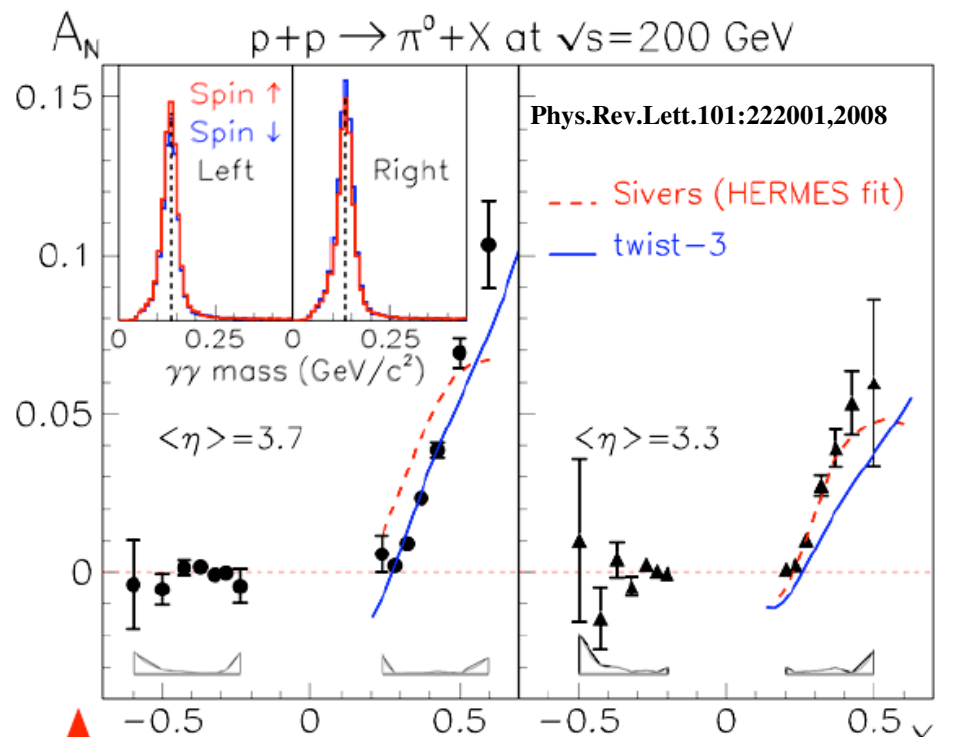

arXiv:0801.2990v1 [hep-ex]

p_T Dependence of A_N in X_F bins

For Fixed X_F, the asymmetry A_N does not fall with p_T as predicted by models, and perhaps expected on very general grounds.

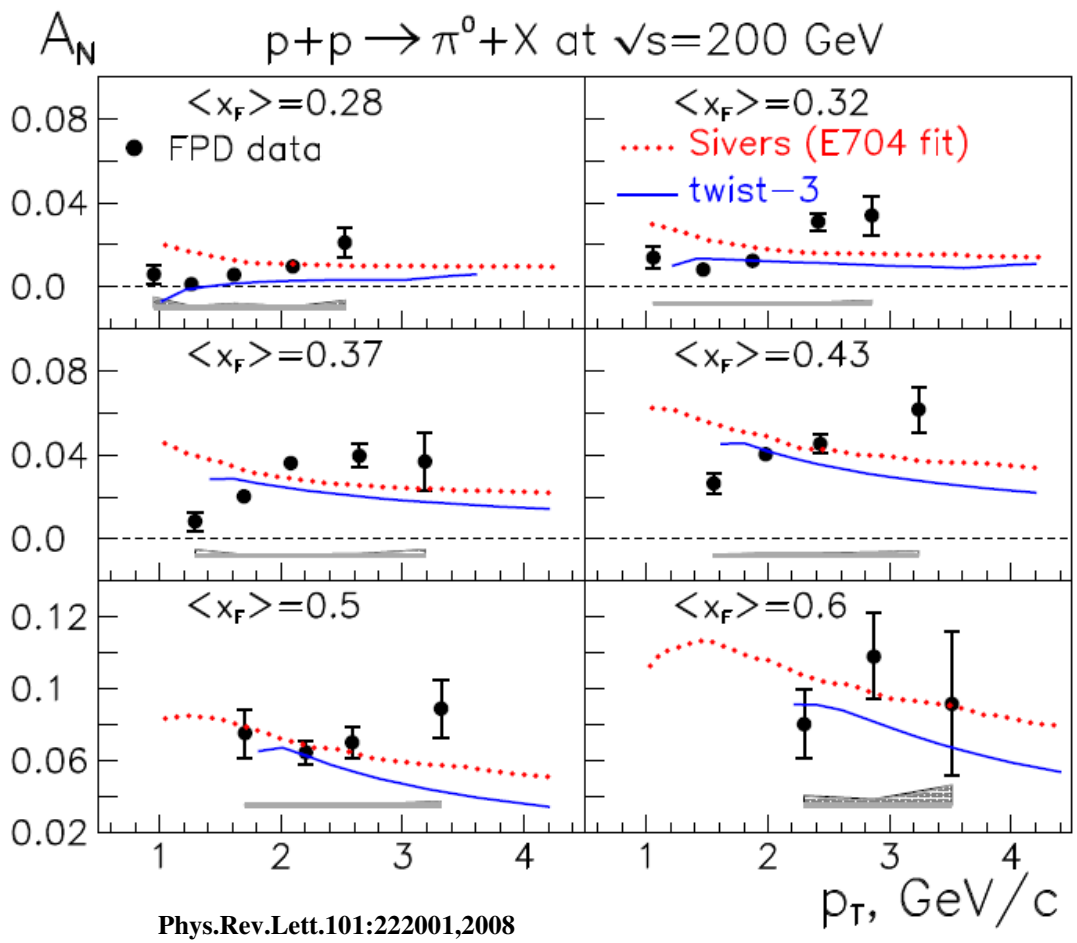

Phys.Rev.Lett.101:222001,2008

U. D'Alesio, F. Murgia, Phys. Rev. D **70**, 074009 (2004).
J. Qiu, G. Sterman, Phys. Rev. D **59**, 014004 (1998).

P_T Dependence in Calculations of A_N

•**Sivers Effect** / **Collins Effect**

•introduce transverse spin dependent **offsets in transverse momentum** ….

•independent of the hard scattering (definition of factorization).

$$P_T \Rightarrow P_T \pm k_T$$

"±" depending on the sign of proton transverse spin direction. **Using our (STAR) measured cross section form:**

$$d\sigma_\uparrow \sim \frac{1}{(p_T - k_T)^6} \qquad d\sigma_\downarrow \sim \frac{1}{(p_T + k_T)^6}$$

$$A_N = \frac{d\sigma_\uparrow - d\sigma_\downarrow}{d\sigma_\uparrow + d\sigma_\downarrow} \sim \frac{6k_T}{p_T} + O\left(\frac{k_T}{p_T}\right)^2$$

Higher Twist Effects:

Qiu and Sterman
Kouvaris et. al. **Phys.Rev.D74:114013,2006**.

A_N Fall as $1/P_T$ as required by definition of higher twist.

All of these models lead to

$A_N \sim\propto 1/P_T$

Phys.Rev.D74:114013,2006.

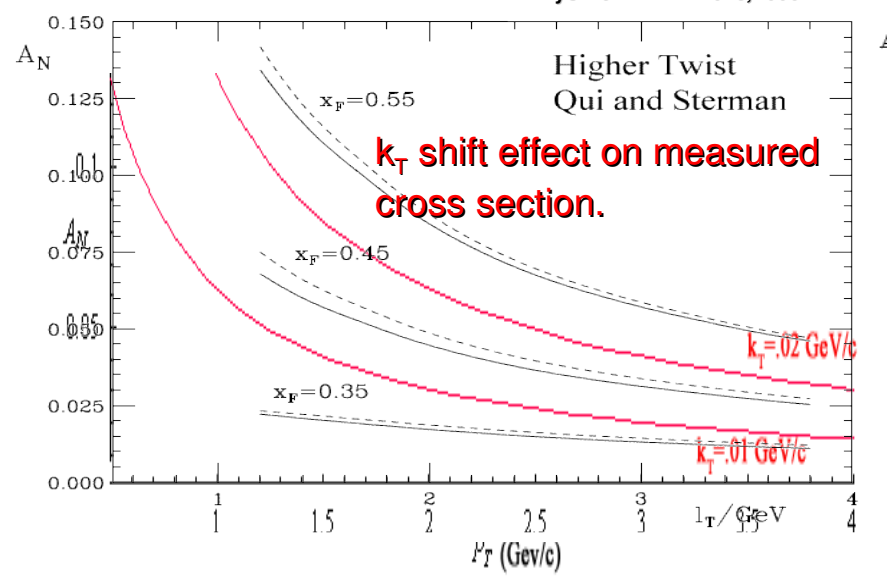

Previous Observation of Transverse SSA Forward Production of Eta Meson by FNAL Exp 704

Nominally (perhaps not significantly) larger asymmetry at high x_F for Eta than π^0. Large Uncertainty in Eta A_N.

$$p_\uparrow + p \rightarrow M + X$$
$$\bar{p}_\uparrow + p \rightarrow M + X$$

$$A_N = \frac{d\sigma_\uparrow - d\sigma_\downarrow}{d\sigma_\uparrow + d\sigma_\downarrow}$$

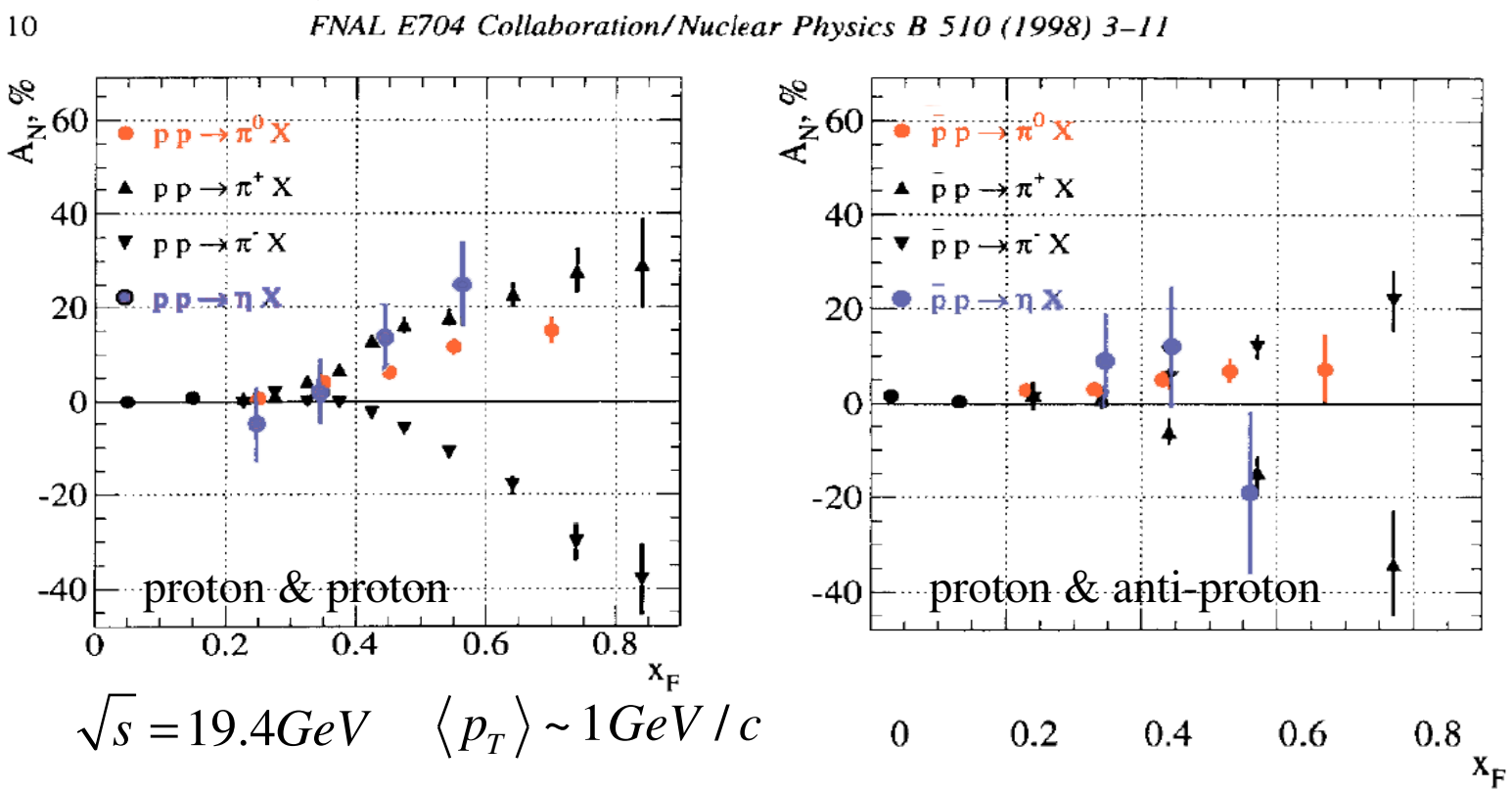

$$\sqrt{s} = 19.4 GeV \qquad \langle p_T \rangle \sim 1 GeV/c$$

Eta Signal in Run6 FPD

Di-Photon Invariant Mass Spectra in 3 Energy Bins

- Center Cut
- 3 columns for 3 energy bins
- Each column shows a single plot in log and linear scale.

π^0 Mass Cut

$.085GeV < M_{\gamma\gamma} < .185GeV$

Eta Mass Cut

$.48GeV < M_{\gamma\gamma} < .62GeV$

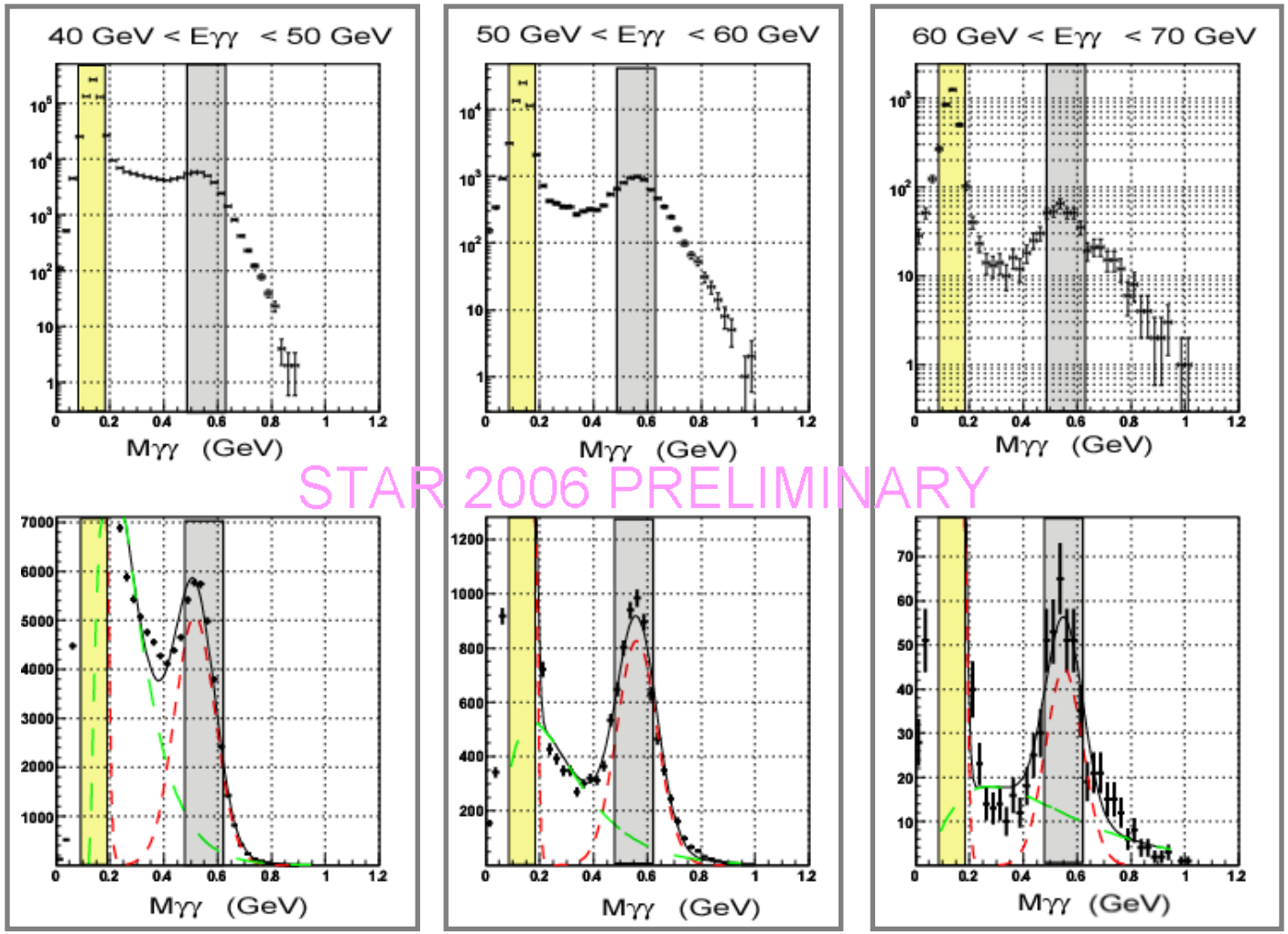

$A_N(x_F)$ will be reported for di-photon events in these two shaded mass regions. We will not separate contributions from backgrounds under the Eta and π^0 peaks.

Mass Dependence of A_N

$$p_{\uparrow} + p \rightarrow M + X$$
$$M \rightarrow \gamma + \gamma \qquad \sqrt{s} = 200\,GeV$$

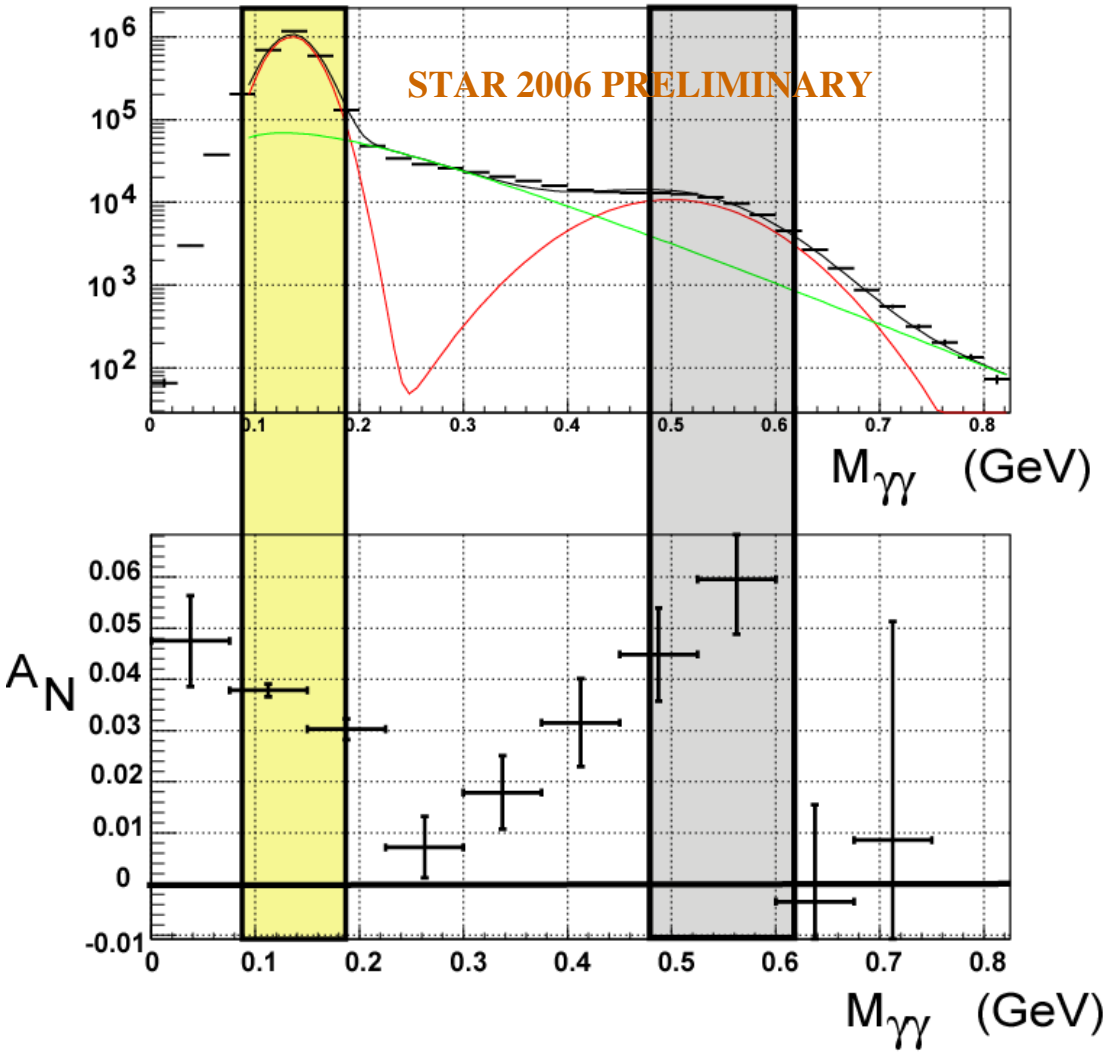

1. $N_{photon} = 2$
2. $E_{total} > 40GeV$
3. No Center Cut
4. Average Yellow Beam Polarization = 56%

- Yellow beam asymmetry clearly reveals the shape of two mass resonances.

- There is an "asymmetry valley" in between π^0 and Eta mass regions.

$A_N(x_F)$ in π^0 and Eta Mass Regions

$$p_\uparrow + p \rightarrow M + X$$
$$M \rightarrow \gamma + \gamma \quad \sqrt{s} = 200\,GeV$$

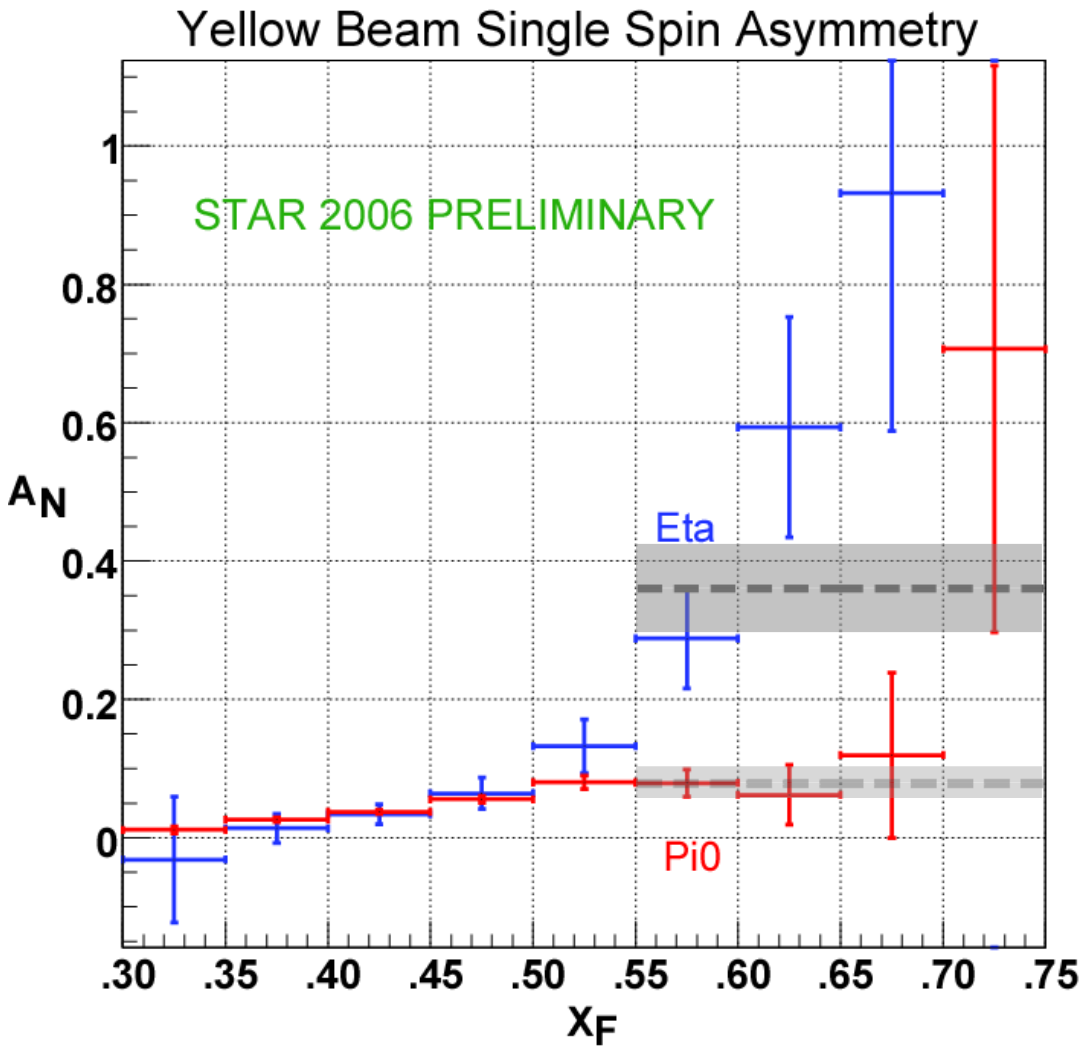

1. $N_{photon} = 2$
2. Center Cut (η and ϕ)
3. Pi0 or Eta mass cuts
4. Average Yellow Beam Polarization = 56%

$$.55 < X_F < .75$$

$$\langle A_N \rangle_\eta = 0.361 \pm 0.064$$

$$\langle A_N \rangle_\pi = 0.078 \pm 0.018$$

For $.55 < X_F < .75$, the asymmetry in the Eta mass region is greater than 5 sigma above zero, and about 4 sigma above the asymmetry in the π^0 mass region.

Should A_N be larger for η than π^0 ?

- **Gluons** or **η** has **Isospin I=0**.
- **u quark** has **Isospin I=1/2**
- **π^0** has **Isospin I=1**.

- But we expect both mesons to come from **<u>fragmentation of quark jets</u>**.

$$I=0 \quad \begin{cases} \eta = \frac{1}{\sqrt{3}}(u\bar{u}+d\bar{d}-s\bar{s}) \\ \eta' = \frac{1}{\sqrt{6}}(u\bar{u}+d\bar{d}+2s\bar{s}) \end{cases}$$

$$I=1 \quad \{ \pi^0 = \frac{1}{\sqrt{2}}(u\bar{u}-d\bar{d})$$

*Assume η, η' mixing angle: $\theta_P \sim -19.5$

- **For Sivers Effect: Asymmetry is in the jet and should not depend on the details of fragmentation.**

- **For Collins Effect**: Asymmetry reflects fragmentation of the quark jet into a leading **η** or **π^0** meson. Differences in fragmentation could relate to:

  - Mass differences?
  - Isospin differences?
  - Role of Strangeness?
  - **But Collins Effect Should be suppressed when Z~1**

Theory Score Card For Factorized QCD Picture for π^0 & η Transverse A_N

✓ Cross Section for Pi0 agrees with PQCD (Normalization and Shape)

✓ Dependence of cross section on X_F and Pt may be similar for Pi0 and Eta at large X_F as expected.

✓ Model calculations (Sivers, Collins, or Twist-3) can explain the X_F dependence of π^0 A_N

X Pt dependence of π^0 A_N.	Inconsistent with $A_N \sim 1/p_T$
? Ratio η / π^0 → nominal 40% - 50%	Yet to be determined.
? Large difference in A_N between π^0 and η	Can Collins or SIvers Model explain it?

Forward π^0 Cross-Section: STAR and ISR

At Large X_F (ie. X_F>0.4) , the π^0 fragment carries most of the of the jet momentum. (<z> > 75%)

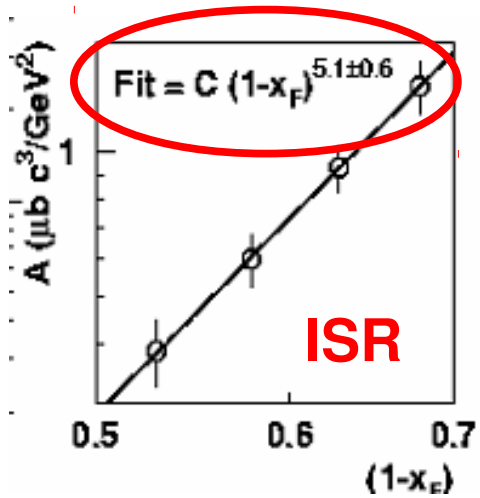

STAR Published Result is similar to
ISR analysis, J. Singh, et al Nucl. Phys. B140 (1978) 189.

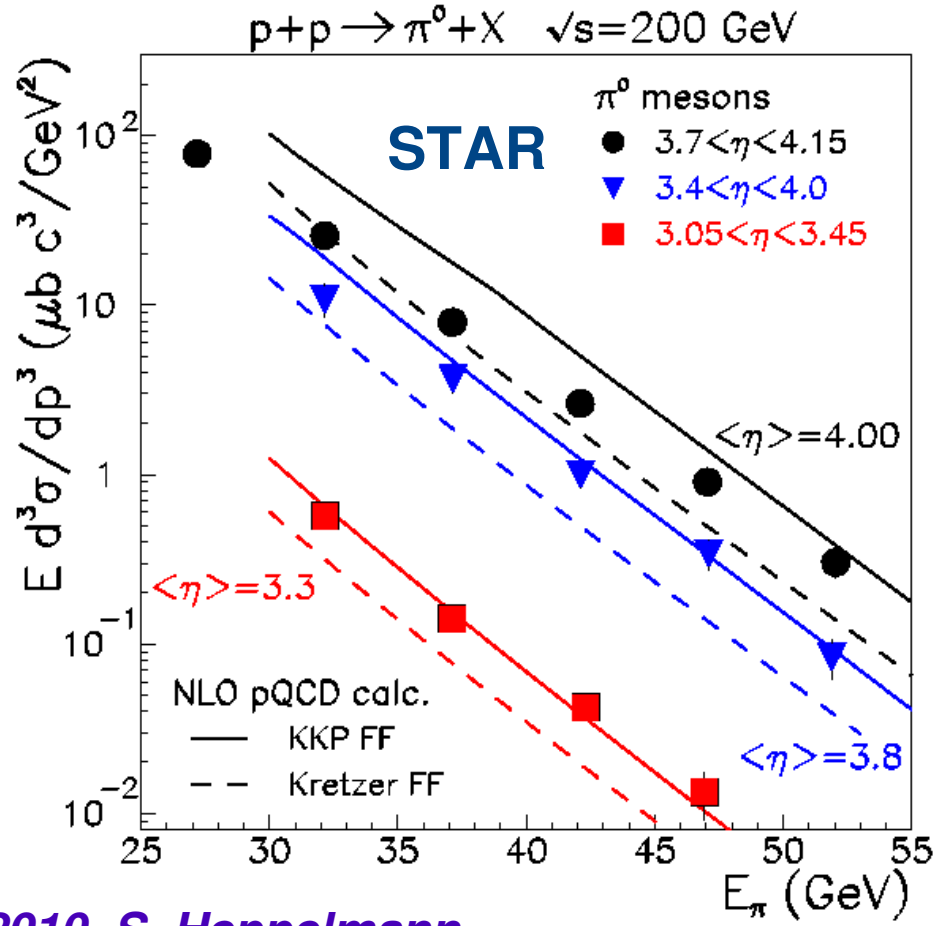

$$E\frac{d^3\sigma}{dp^3} \propto \frac{(1-x_F)^N}{p_T^{-B}}$$

$$N \approx 5 \quad B \approx 6$$

$$e^{\left(\frac{-2(N+B)}{100}E\right)} = e^{\frac{-2\cdot 11}{100}E} = e^{-0.22\ E}$$

$$for\ \ 20\text{GeV} < E < 80\text{GeV}$$

RSC 2010, S. Heppelmann

Alternatives to Factorized PQCD Lead to very different cross sections

- Preliminary look at invariant cross section are likely consistent with conventional

$$\frac{\left(1-x_F\right)^5}{p_T^{\,6}}$$

- In contrast, analysis of low p_T **Regge type processes** lead to **to a different form** for the dependence of the cross section on $(1-x_F)$ as Feynman x_F approach unity.

$$Regge\ Cross\ Section \sim \left(1-x_F\right)^2$$

L.L.FrankFurt and M.I. Strikman, Vol. 94B2 Physics Letters, 28 July 1980.
and Private Communication.

General Issues: Transverse SSA with Factorization in the Context of Collins/Sivers ….

$$P_T = p_T^{\,hard\ scattering} + k_T^{\,Collins/Sivers}$$

$k_T^{\,Collins/Sivers}$ changes sign if proton transverse spin changes sign.

Does $k_T^{\,Collins/Sivers}$ depend upon $p_T^{\,hard\ scattering}$?

By Definition Factorization Implies NO!!!!

$$A_N(P_T) = \frac{\sigma\left(p_T + \langle k_T \rangle\right) - \sigma\left(p_T - \langle k_T \rangle\right)}{2\sigma(P_T)}$$

$$\sim \frac{1}{\sigma}\frac{d\sigma}{dP_T}\langle k_T \rangle$$

pQCD: $\sigma \sim \frac{1}{p_T^{\,6}} \rightarrow A_N \sim \frac{1}{p_T}$

Exponential: $\sigma \sim e^{-k \cdot p_T} \rightarrow A_N \sim const$

So factorization can *imply* a direct relation between p_T dependence of A_N and the p_T dependence of cross section.

pQCD: $\sigma \sim \frac{1}{p_T^{\,6}} \rightarrow A_N \sim \frac{1}{p_T}$

Exponential: $\sigma \sim e^{-k \cdot p_T} \rightarrow A_N \sim const$

In FMS:

p_T dependence

Involves measurement of variation from cell to cell.

Requires all neighboring cells to have accurate gain determination.

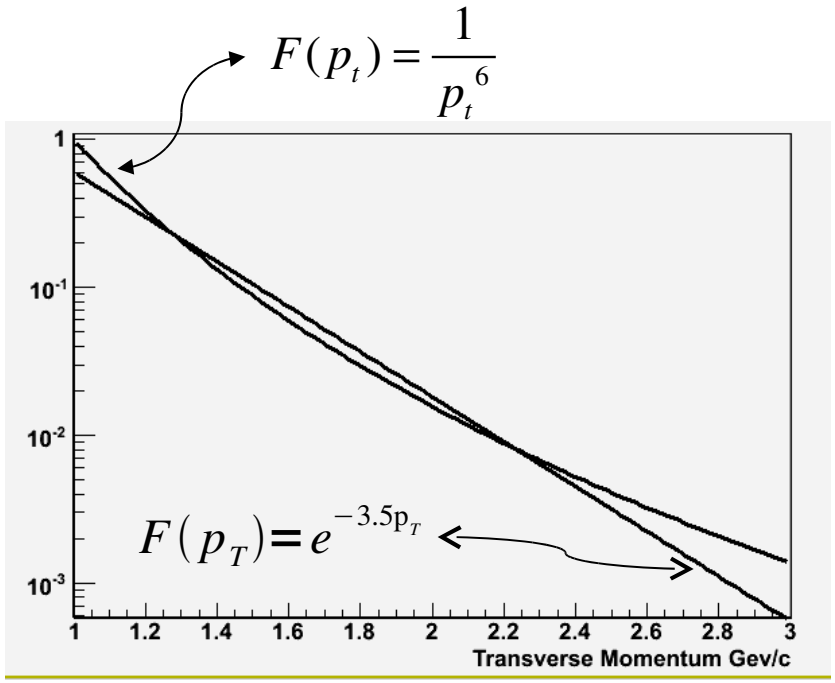

x_F dependence involves energy distribution within one or a few cells

This is opposite in central region!!

STAR Forward Meson Spectrometer (FMS)

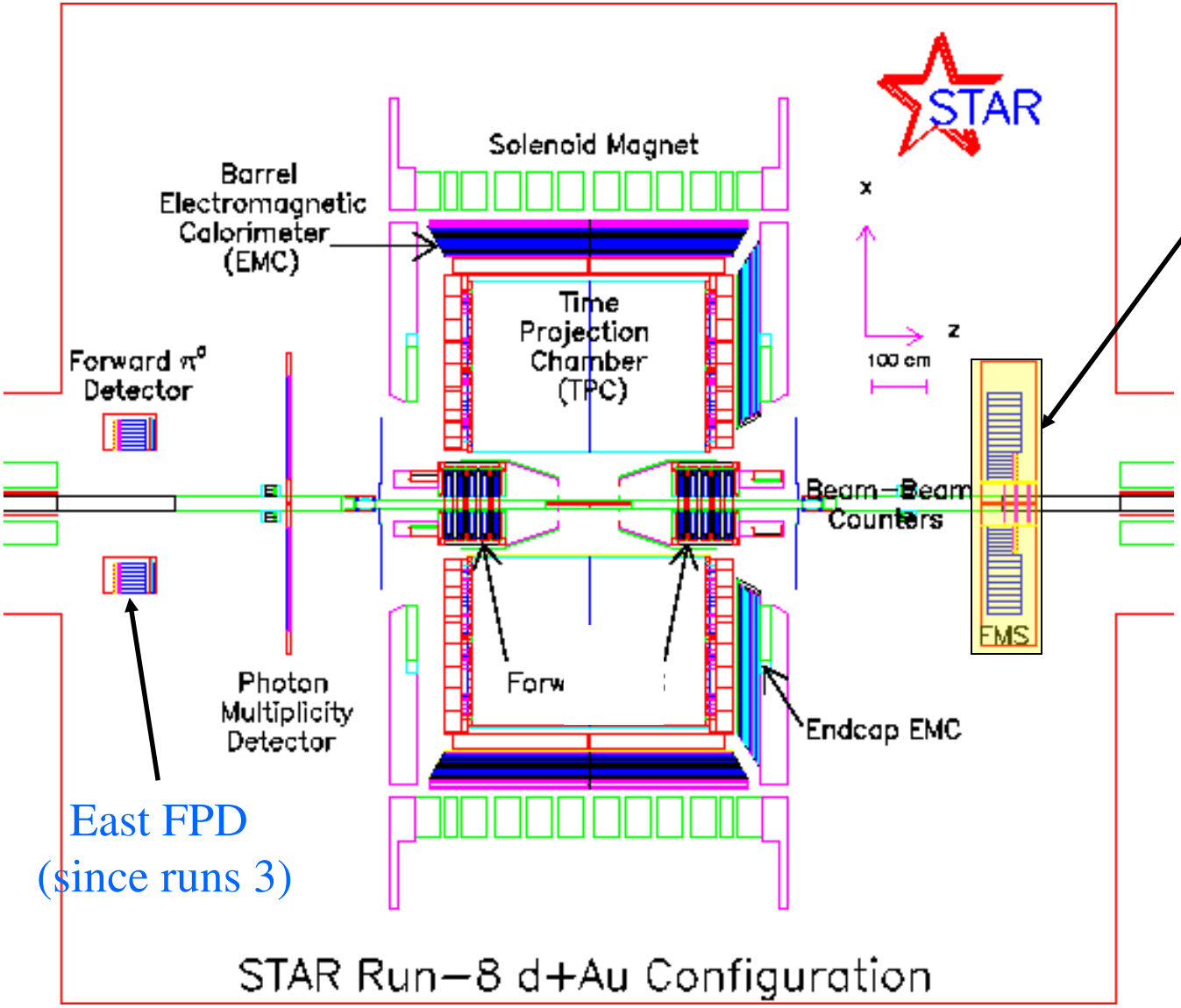

East FPD
(since runs 3)

Since Run 8:
FMS

- Stack of 1264 lead glass cells, roughly 18 X_0 in z.
- Located at far West side of Hall, at the opening to RHIC tunnel. Faces blue beam.
- 7.5 meters from interaction point

FMS Greatly Enhances STAR EM Coverage

- EMC Calorimeters
  - bEMC -1<η<1
  - eEMC 1<η<2
  - FMS 2.5<η<4
  - FPD movable
- Tracking
  - TPC
  - FTPC

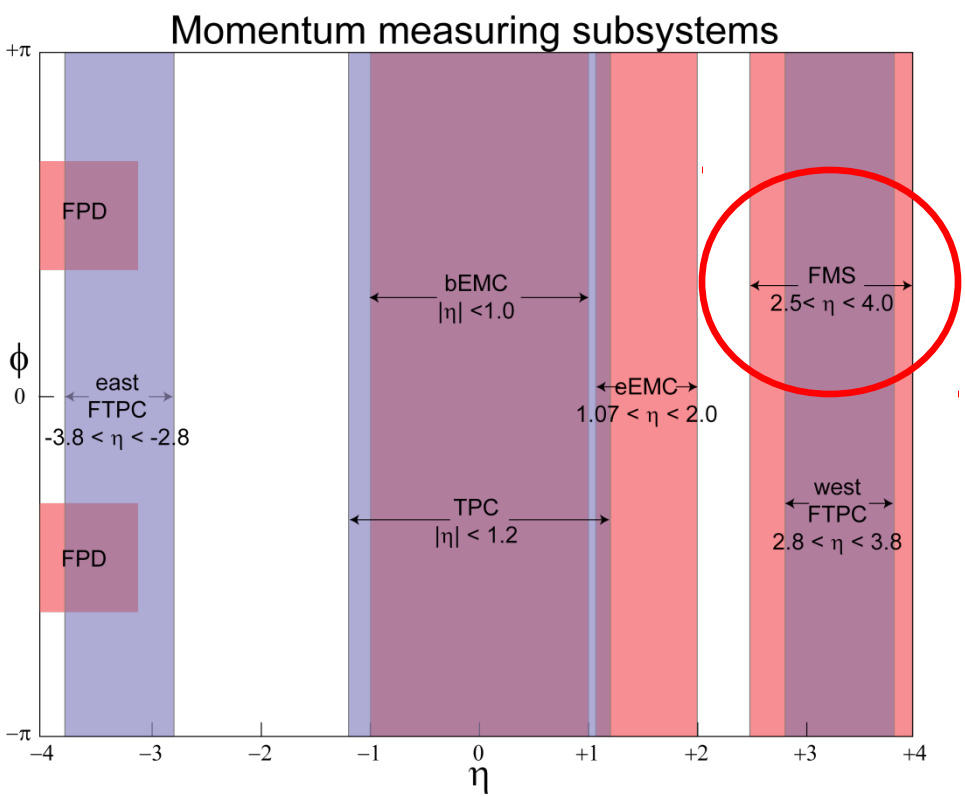

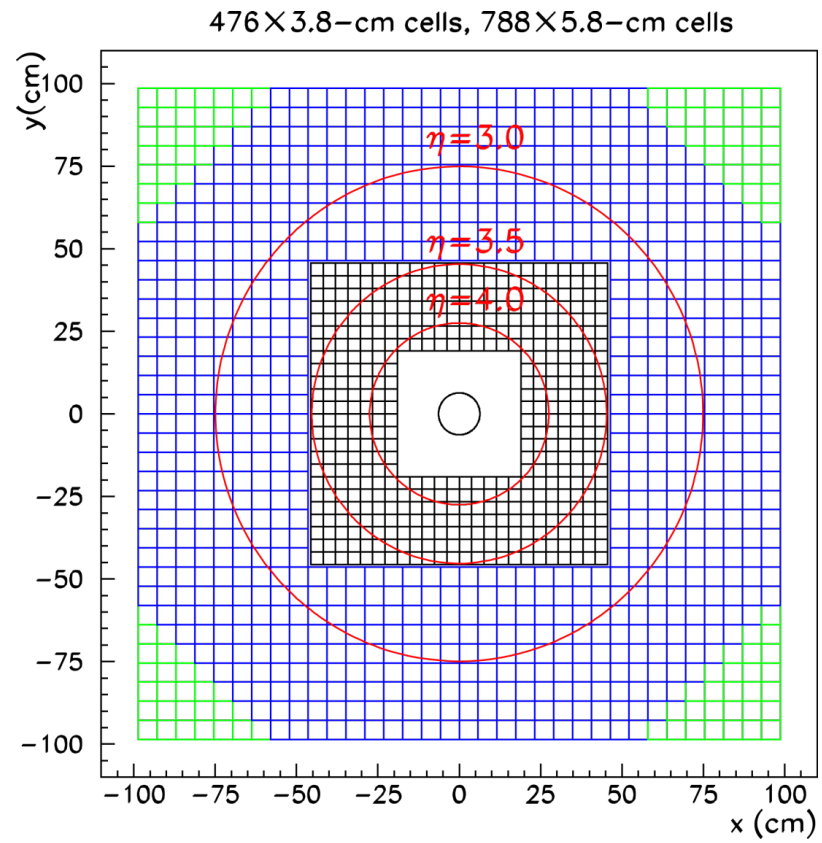

With installation of FMS, STAR EM calorimeter coverage spans most of the pseudo-rapidity region from -1<η<4.

Forward Meson Spectrometer

Lead Glass From FNAL E831
804 cells of 5.8cm×5.8cm×60cm
Schott F2 lead glass

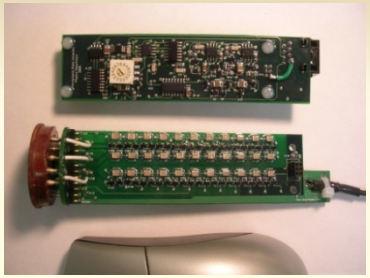

Small Cell PSU Type 224 of 476

Cockcroft-Walton HV bases with computer control through USB. Designed/built in house for FEU-84.

Designed and built at Penn State University

QT board

Readout of 1264 channels of FMS provided by QT boards. Each board has

- **32 analog inputs**
- **5-bit TDC / channel**
- **Five FPGA for data and trigger**
- **Operates at 9.38 MHz and higher harmonics**
- **Produces 32 bits for each RHIC crossing for trigger**
- **12-bit ADC / channel**

Designed and built at UC Berkeley/SSL

Preliminary Run8 FMS π^0 A_N

Azimuthal Angle Dependence of A_N

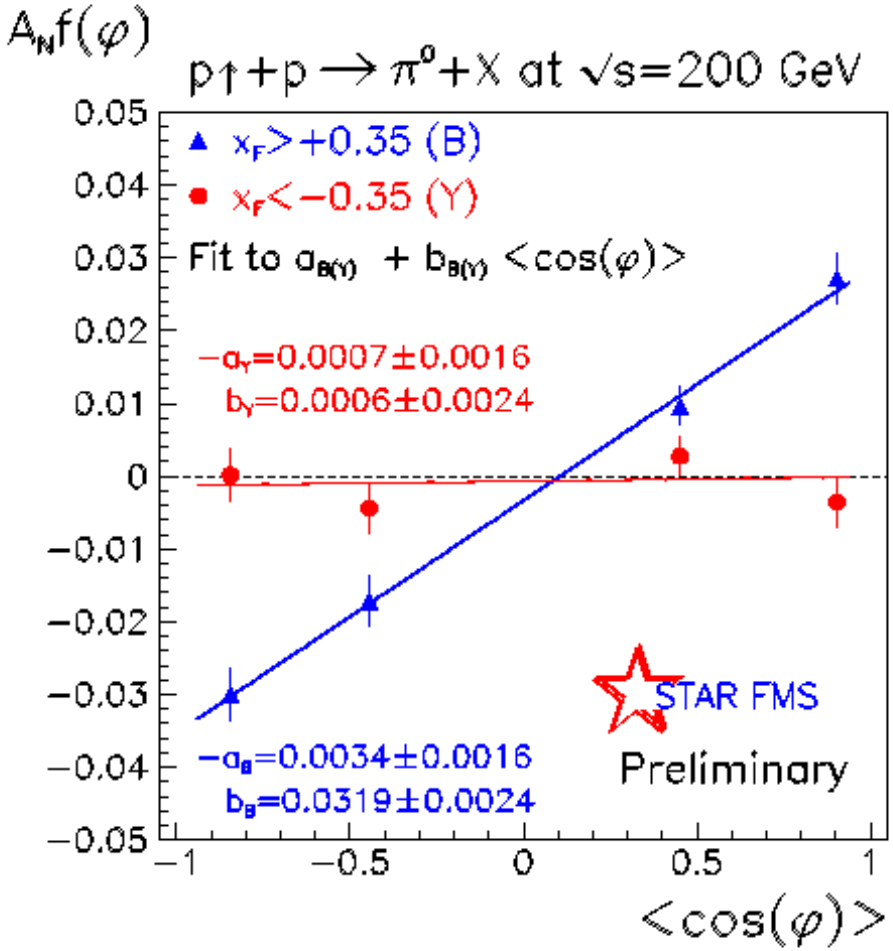

A_N vs. xF

→ Consistent with previous measurements

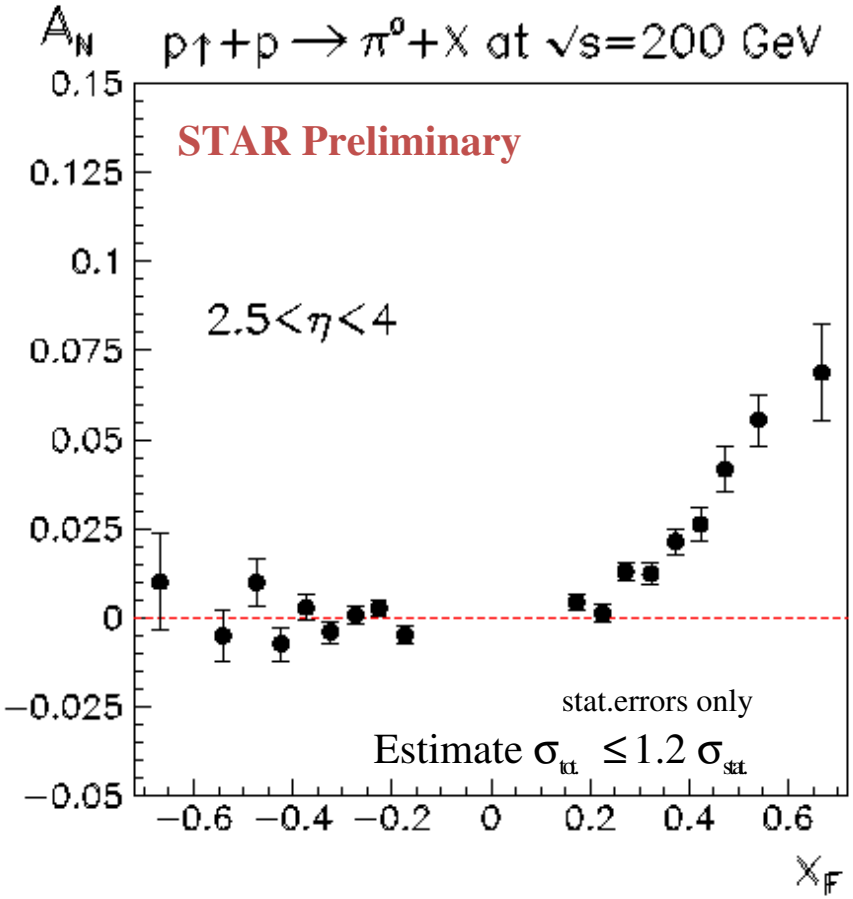

From SPIN08 talk by N. Poljak, arXiv:0901.2828

p_T-dependence of π^0 A_N

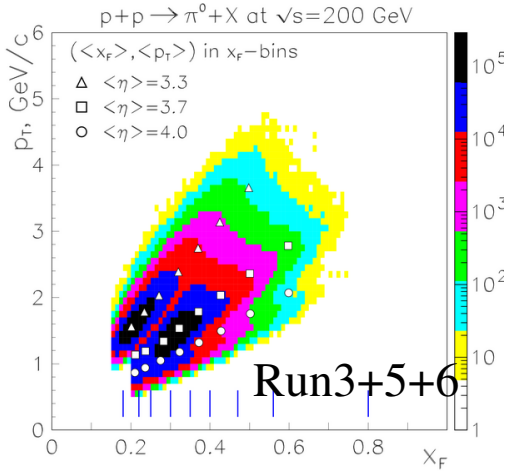

Large solid angle of the FMS allows simultaneous mapping of x_F vs p_T with greater statistics

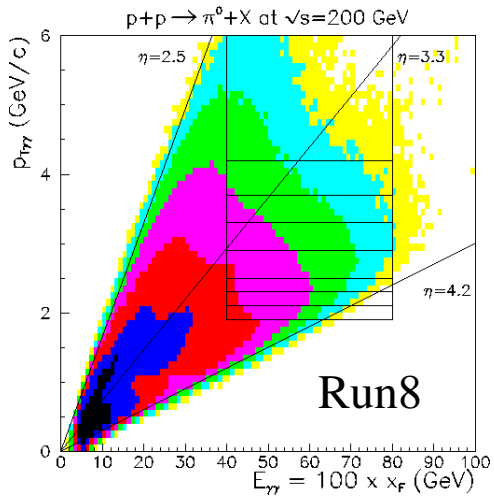

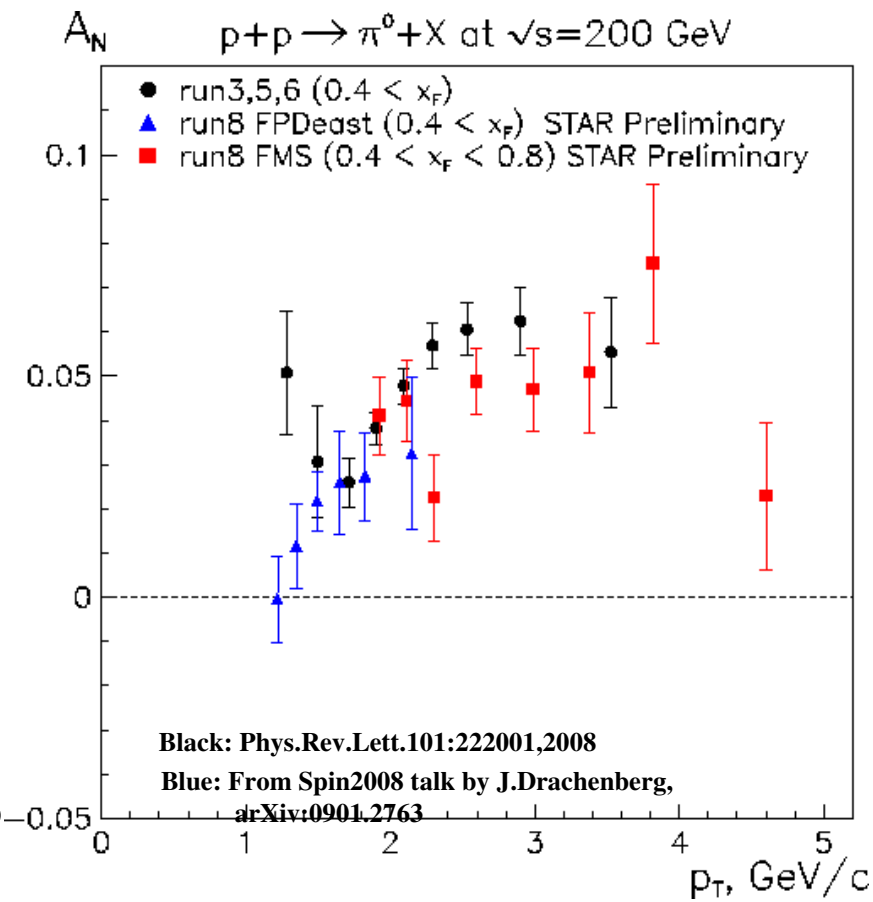

F.o.M. was smaller in run8 than in run6

→ More statistics needed

FMS Calibration for Run 9 and Beyond

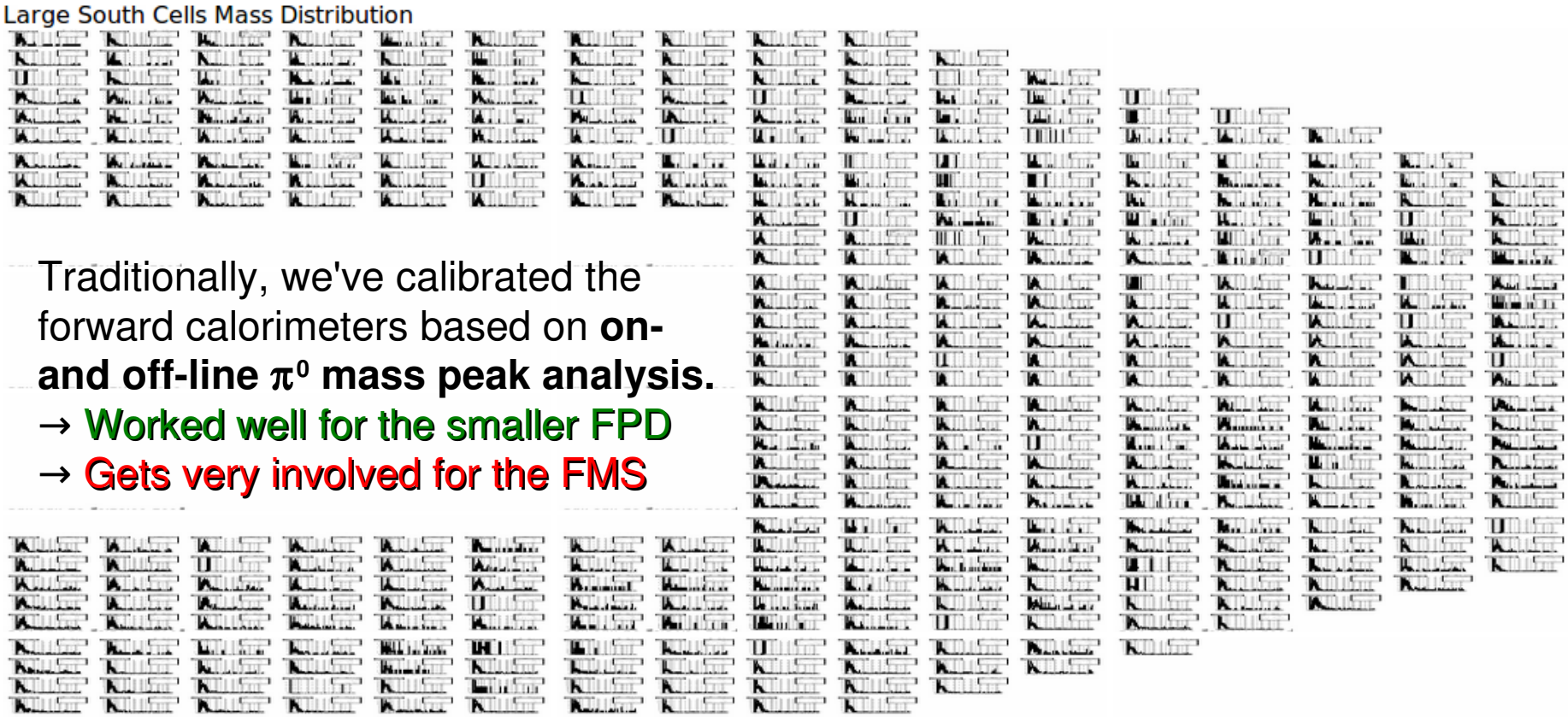

Traditionally, we've calibrated the forward calorimeters based on **on- and off-line π^0 mass peak analysis.**

→ Worked well for the smaller FPD

→ Gets very involved for the FMS

With the much larger FMS, (2x49 channels → 1264 channels) the on-line calibration based on π^0 analysis can be too time consuming.

Bigger detector also brings in more features, such as dead cells and edges. It has been known that the π^0 mass analysis can sometimes find local false solutions, especially in the vicinity of dead cells.

New Trigger Rate Based Calibration

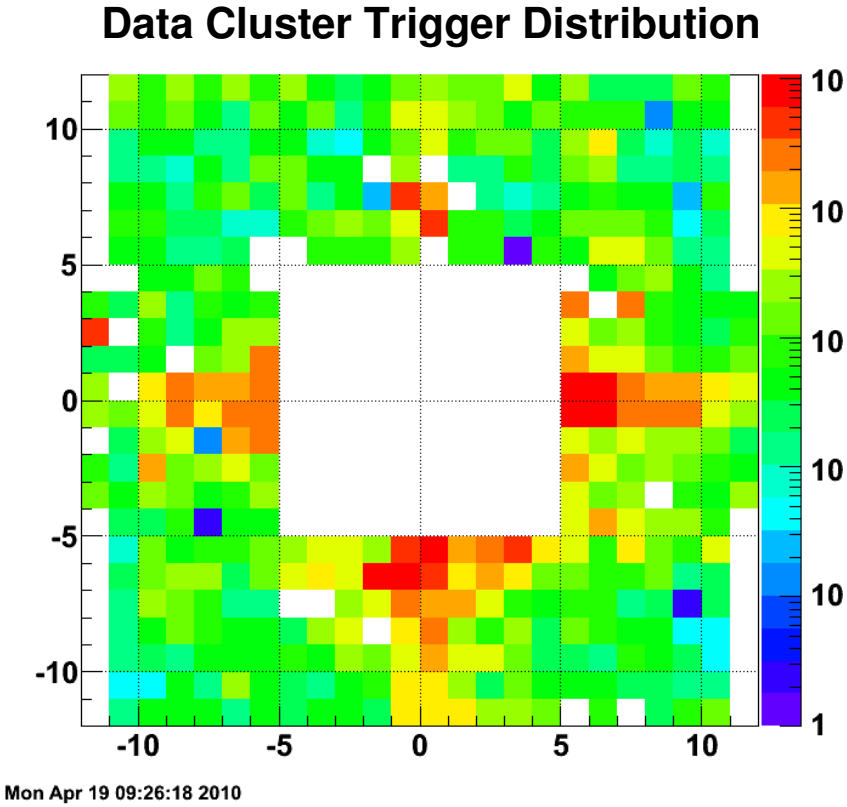

For the run 9 off-line calibration, **we are implementing a trigger-rate based calibration method** that compliments the existing π^0 mass analysis.

Software emulation of run 9 cluster trigger was found to match the data very well.

Based on preliminary gain, we can calculate the simulated trigger rate using Pythia + GSTAR, and compare that with real data trigger rate to get new desired gain → Iteration

Now we have two independent methods of calibration that compliment each other.

- No reconstruction → The on-line calibration time can be substantially reduced
- Works better around dead cells and edges
- Detailed trigger simulation can be used to set up the FMS trigger for future runs

Run 9 FMS Calibration Continues

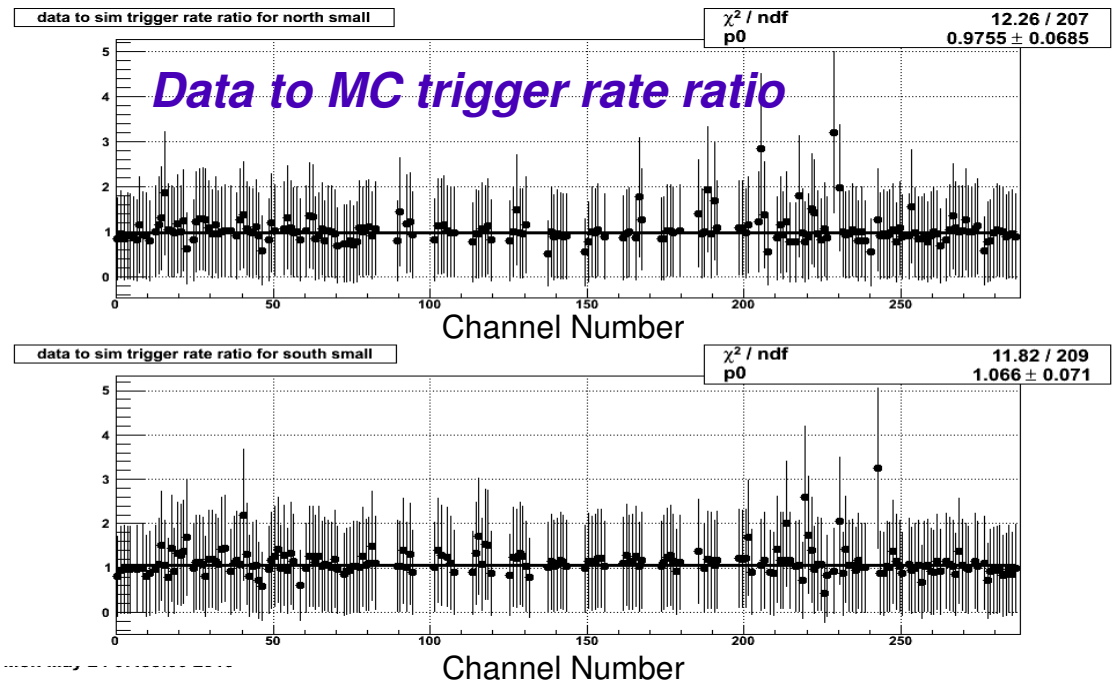

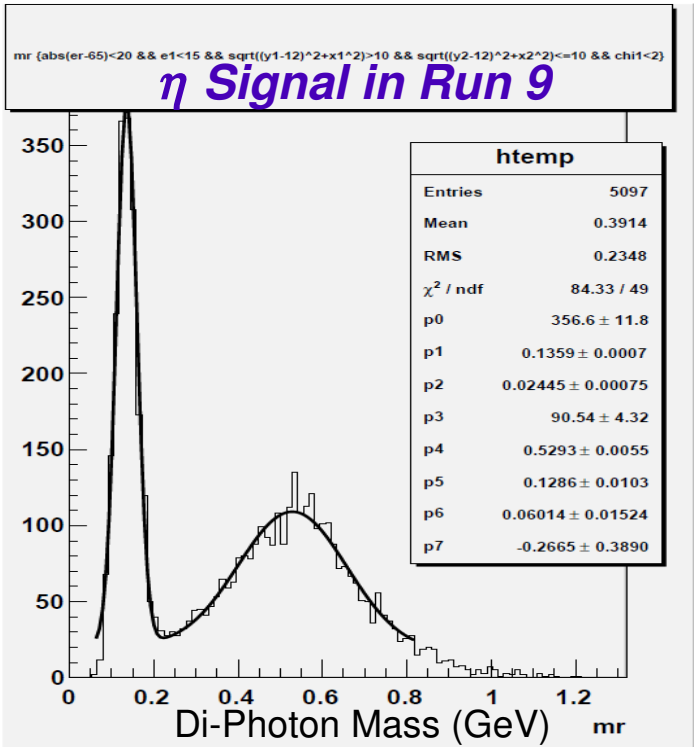

- Preliminary results from the mass-trigger combined calibration scheme for the FMS are promising
- Continual work on the calibration and the FMS run 9 data analysis is ongoing
- We will continue to work on the large cells

Projected SSA Errors for 20pb^{-1} 500GeV Run

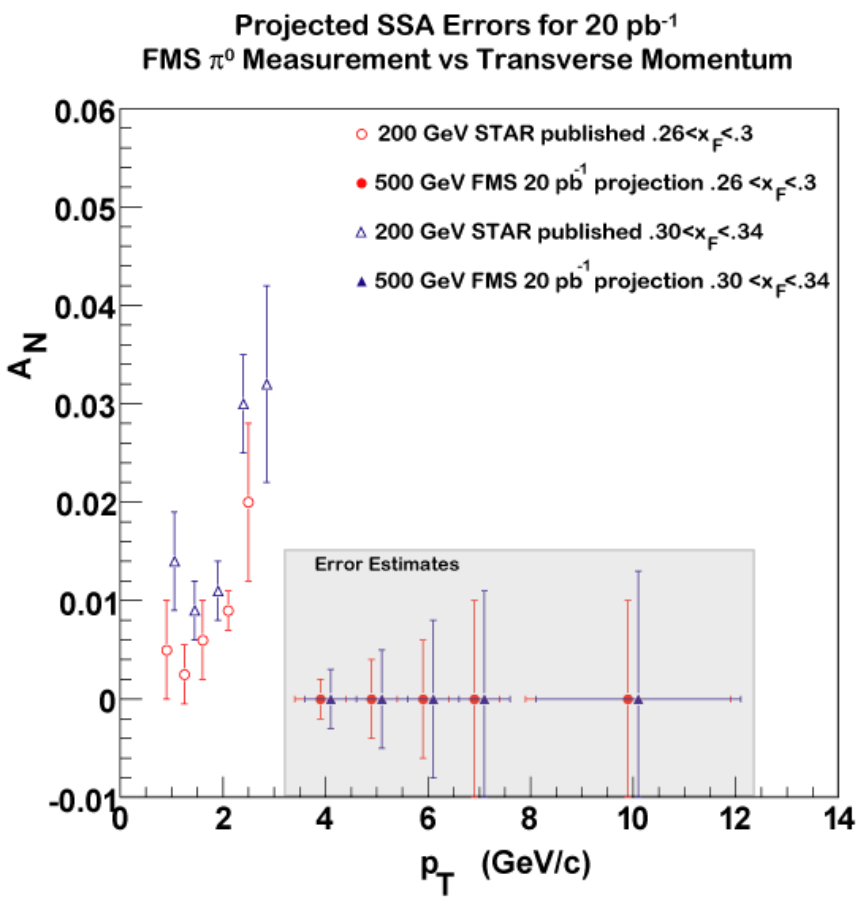

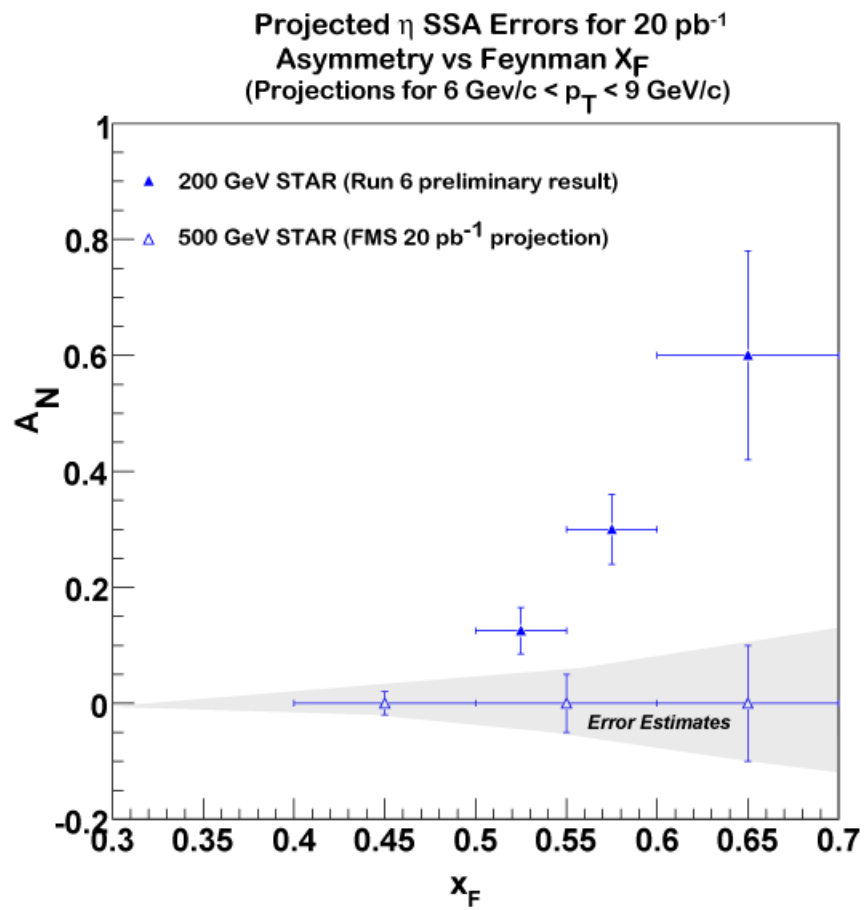

Mid-Rapidity Collins Asymmetry

Φ_π = Azimuthal angle of the pion relative to the jet reaction plane

Φ_S = Azimuthal angle of the proton spin relative to the jet reaction plane

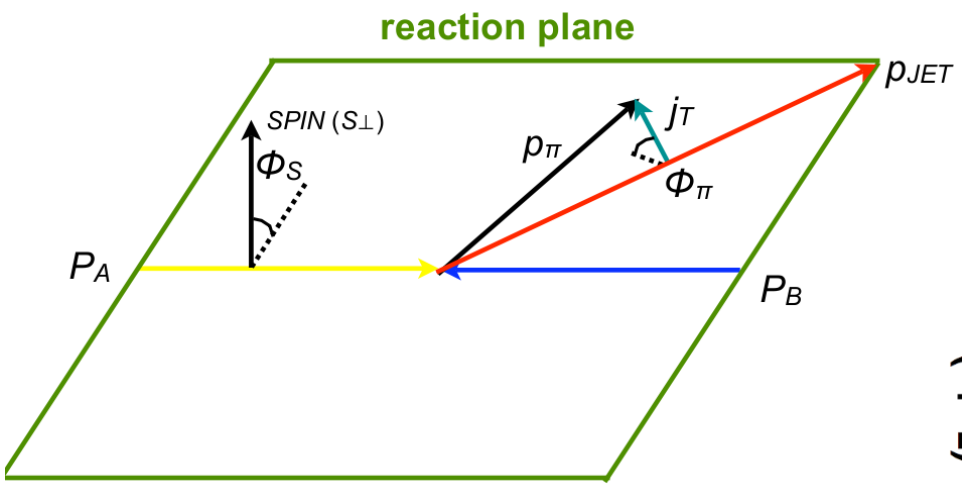

With Collins mechanism, the asymmetry comes from the **quark spin dependent fragmentation.**

$$A(z, j_T) = \frac{\sum \sin(\phi_\pi - \phi_S)}{N}$$

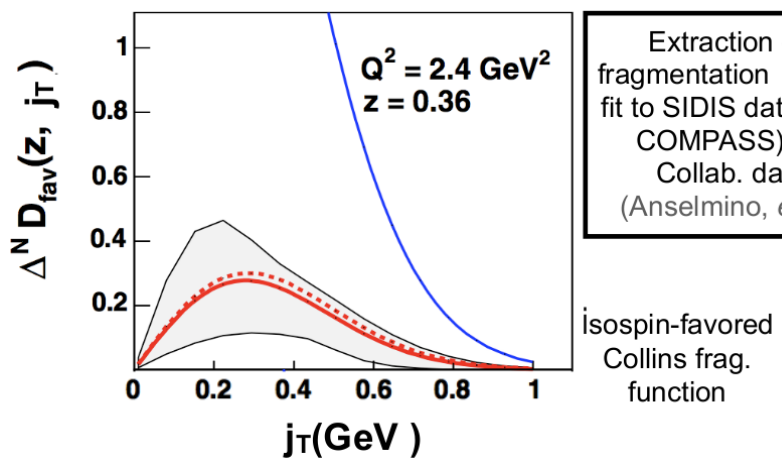

Extraction of Collins fragmentation function from fit to SIDIS data (HERMES, COMPASS) and Belle Collab. data (KEK) (Anselmino, *et al.*, 2008)

isospin-favored Collins frag. function

Here, **we measure the asymmetry in charged pion production with respect to the jet axis** as a function of momentum fraction z and jet transverse momentum j_T.

Predicted Asymmetry (estimate): $A(\pi^\pm) \approx 0.03$

Mid-Rapidity Collins Asymmetry

Charged pions from TPC
(momentum and dE/dx, Min. 25 fit points)
→ Only leading pions are kept.

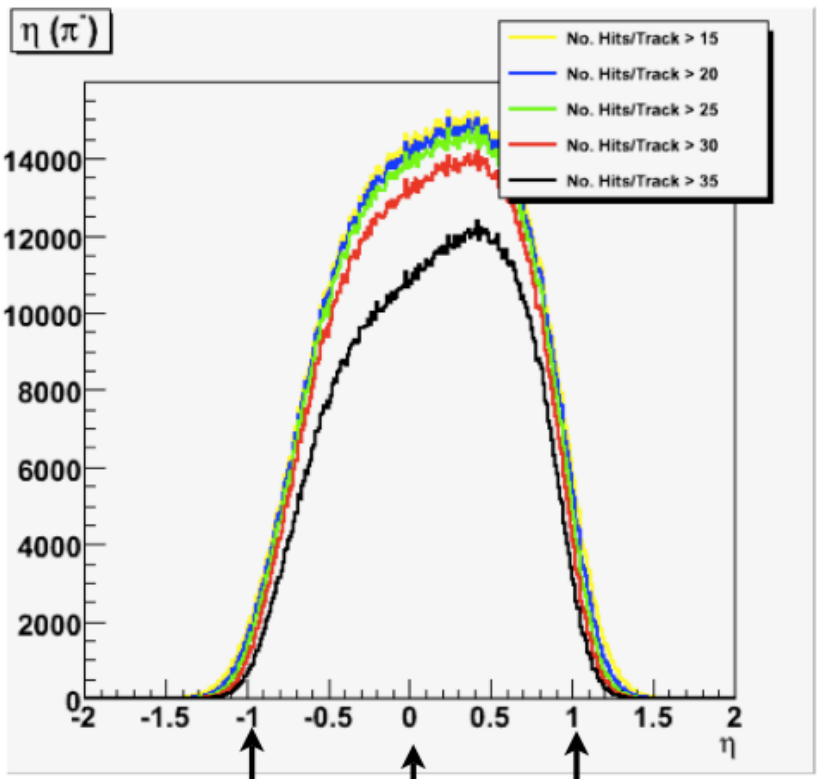

backward BEMC, TPC edge

90°

forward BEMC, TPC edge

Jets from BEMC
→ Jet Patch and High Tower triggers

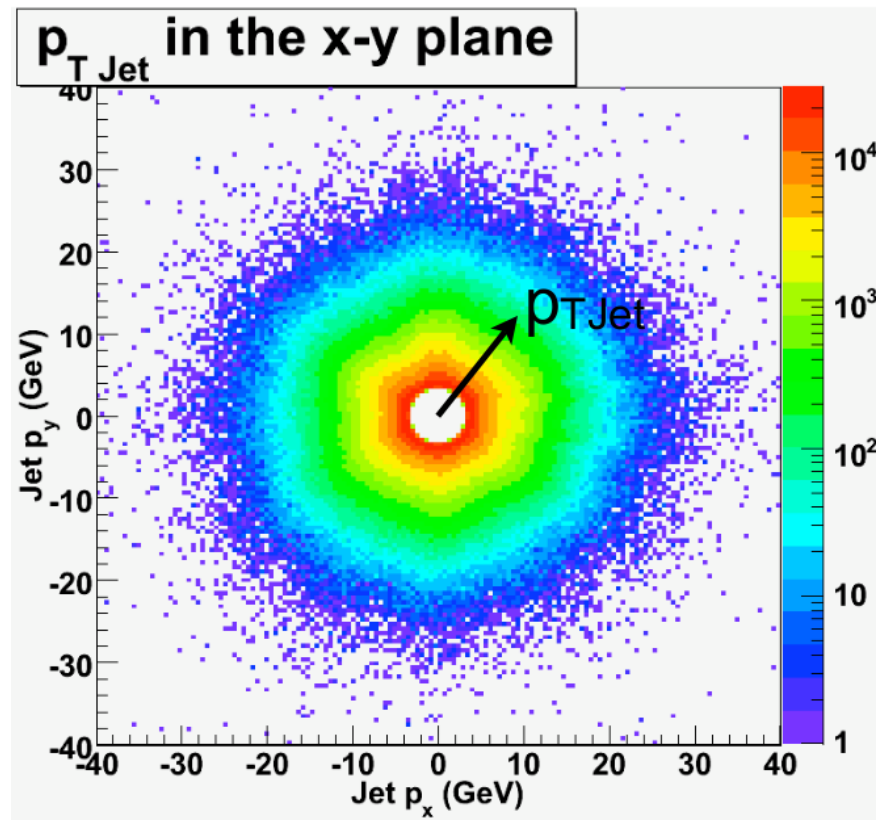

Full Azimuthal Angle Coverage

Analysis in Progress

$\sin(\Phi_S - \Phi_\pi)$ Spectrum

Red = ↑ , Black = ↓ (lab frame pol.)

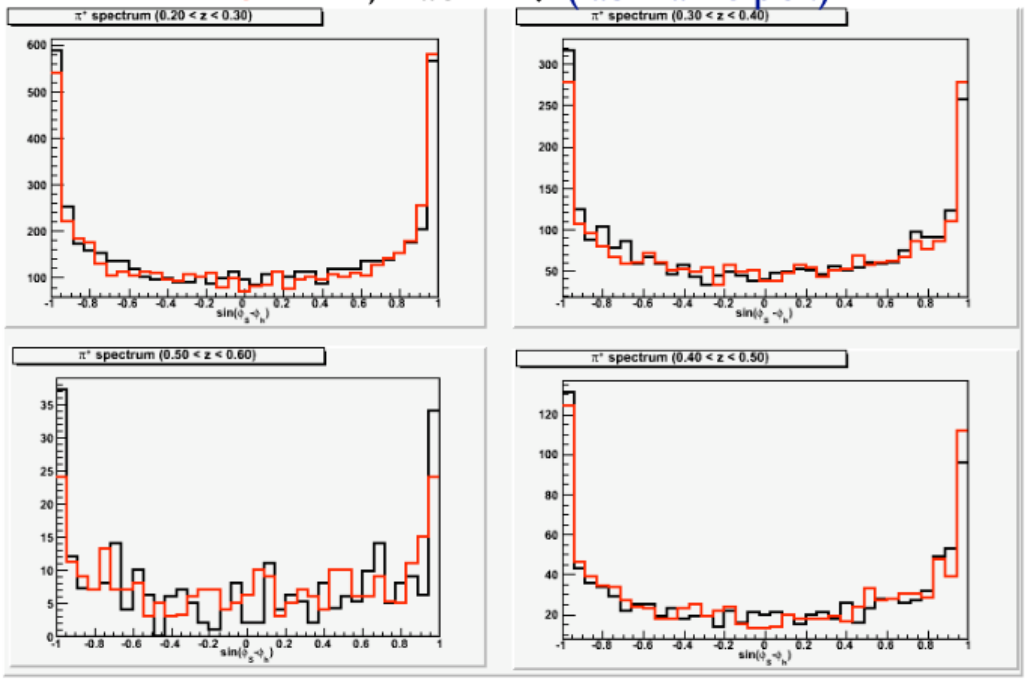

(Use of opposing polarizations, weighted by beam luminosity, ensures that detector acceptances cancel in the asymmetry.)

Jets in the forward hemisphere of each beam are analyzed.

Asymmetry should be opposite in sign for π^+ and π^-

Asymmetry Statistics

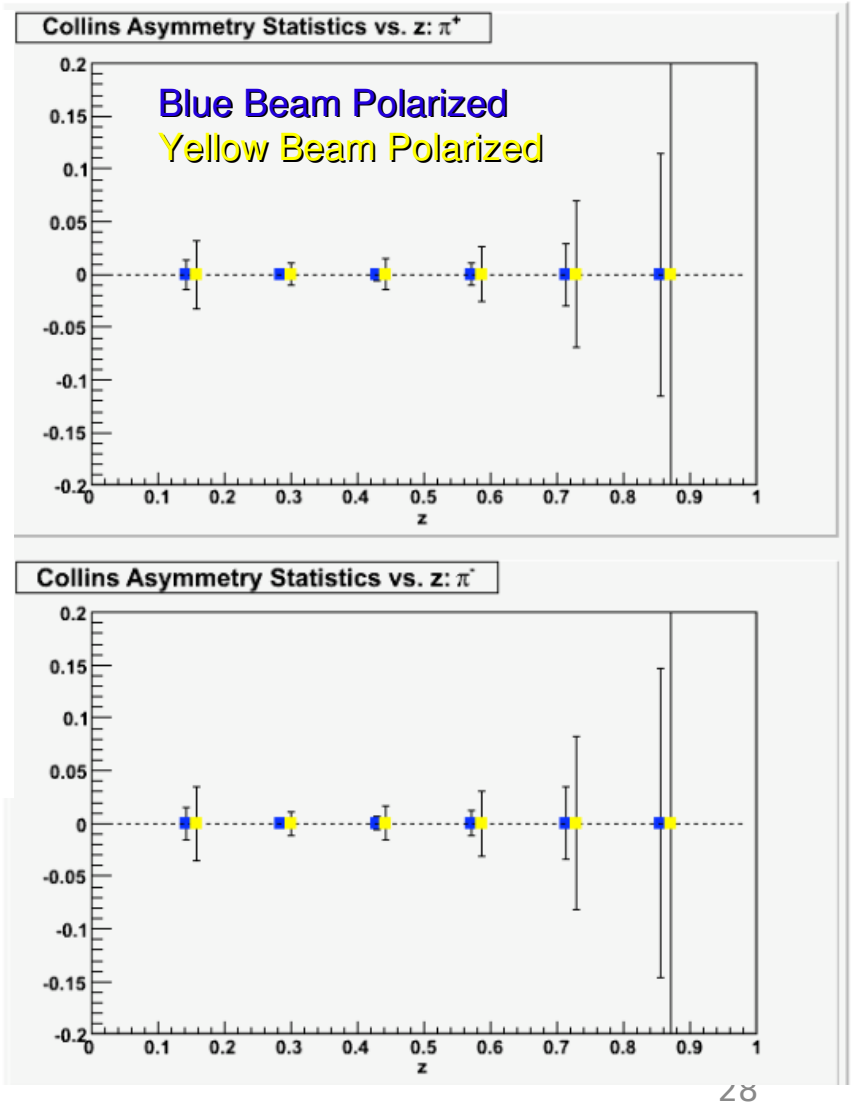

Summary

- From RHIC run3 to run8, the FPD measured large forward single spin asymmetry, A_N, for π^0. The x_F dependence of A_N was qualitatively consistent with theoretical predictions. p_T dependence, however, differed significantly from predictions based on all currently existing models

- In addition to π^0, Eta mesons were observed in the east FPD during RHIC run6. We measured the single spin asymmetry in the π^0 and the Eta mass regions, at $<\eta>\sim3.65$ and x_F above 0.4. We found the A_N in Eta mass region to be ~4 standard deviation greater than the A_N in π^0 mass region from 55GeV to 75GeV. (x_F=0.55~0.75)

- Factorization implies that there is a link between the p_T dependence of the cross-section, and the observed magnitude of the single spin asymmetry. Forward Meson Spectrometer (FMS), commissioned in RHIC run 8, can provide STAR with an opportunity to explore this connection.

- The preliminary results from run 8 FMS show that π^0 $A_N(x_F)$ is consistent with previous measurement, while the azimuthal angle dependence of A_N is as expected.

- The off-line calibration of the run 9 FMS data is well under way. The newly implemented trigger-rate method, based on the careful simulation of the cluster trigger algorithm, compliments the existing invariant mass based calibration, and promises to improve both on- and off-line calibration for the future FMS data taking.

- Mid-rapidity Collins asymmetry analysis based on run 6 data is in progress. Collins mechanism provides sensitivity to the quark transversity in polarized proton collisions.

Run6 FPD Acceptance for π^0 and Eta

Fast Simulator

The ratio of N(reconstructed particles) to N(generated particles with CoM within FPD)

$$m_{\gamma\gamma} = E_{tot}\sqrt{1-(Z_{\gamma\gamma})^2}\,Sin\frac{\theta}{2} \qquad z_{\gamma\gamma} = \frac{E_{\gamma 1}-E_{\gamma 2}}{E_{\gamma 1}+E_{\gamma 2}}$$

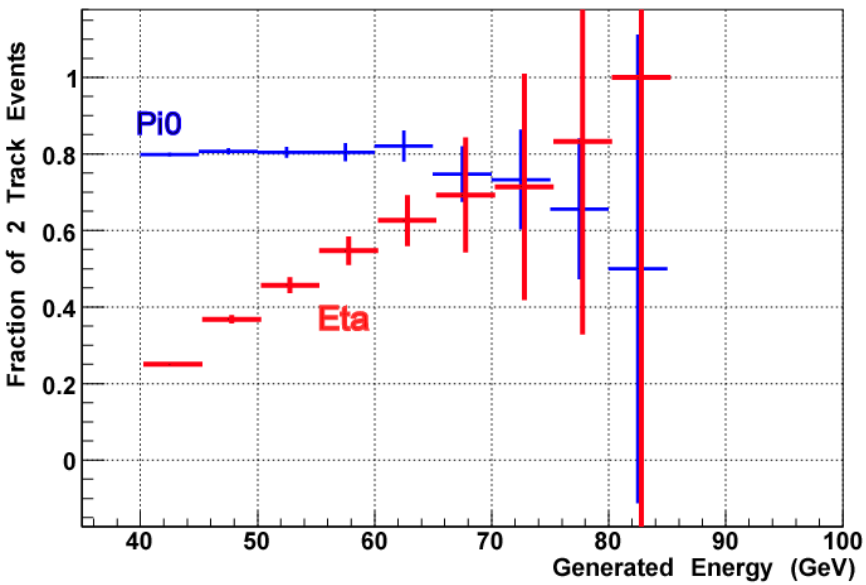

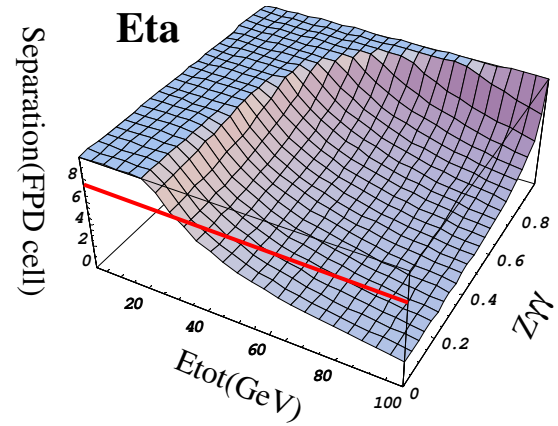

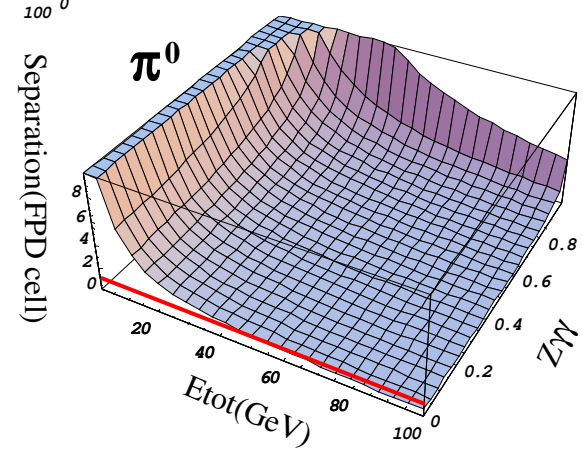

- 7x7 FPD has limited acceptance for Eta mesons. At 40GeV, a symmetrically decaying Eta needs to point to the center of the FPD to fit in. Acceptance improves greatly at higher energy.
- π^0 reconstruction efficiency starts to drop over 60GeV, where the separation between two photons for symmetric decay becomes on average less than 1 cell width.

New Run 9 FMS Calibration - Details

Software emulation of run 9 trigger was found to match the data trigger response very well.

Cell-by-cell trigger rate is determined by π^0 (or photon) cross section and cell gain

Assume trigger rate is a function of gain as: $tr = exp(A_0+A_1*gain)$

Based on some preliminary gain, we can calculate the simulated trigger rate using Pythia + GSTAR, and compare that with real data trigger rate to get new desired gain

Gain correction factor from π^0 mass and from trigger rate are added together with equal weight to calculate the new gain. This calibration process brings both the trigger rate and Pi0 mass to the desired position

Pi0 Mass in Energy Bins

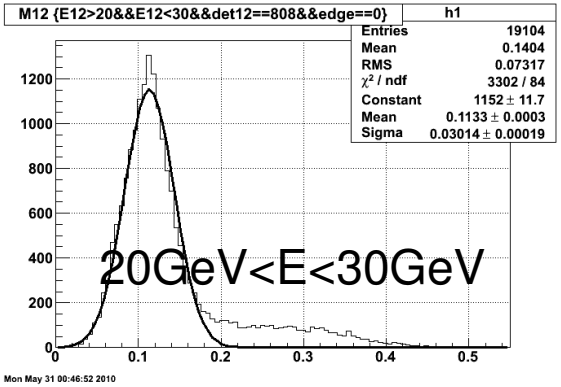

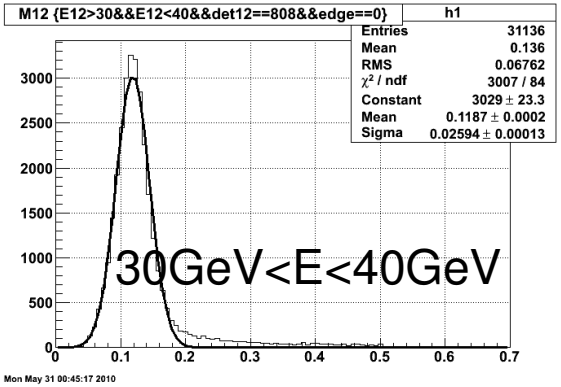

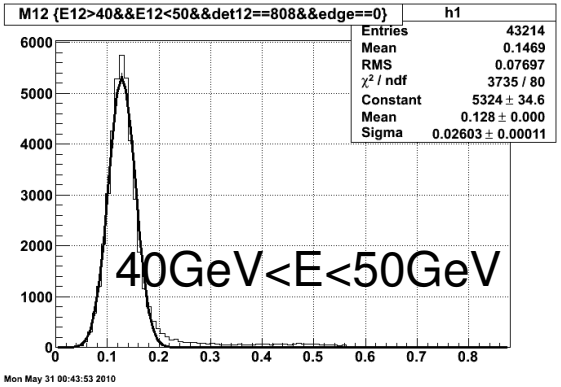

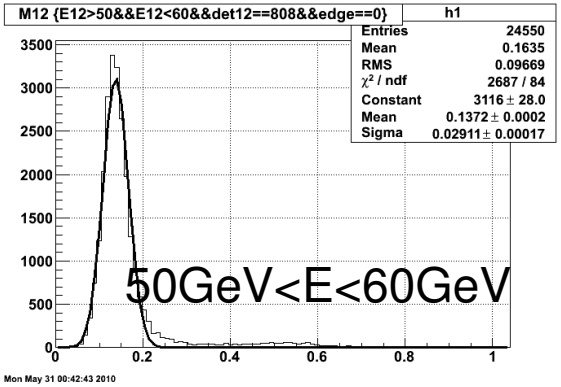

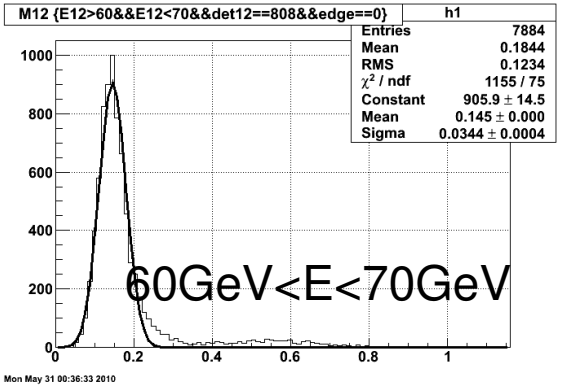

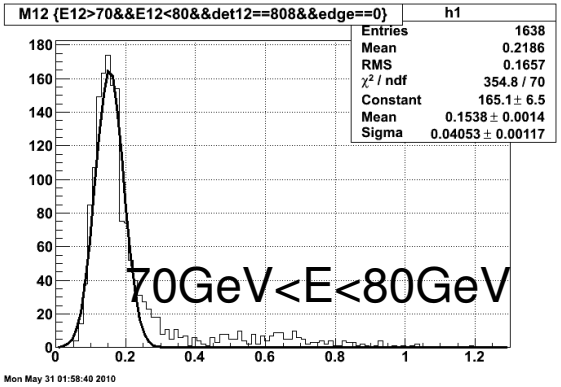

- Pi0 mass shift is ~7% per 10 GeV in energy
- About 3% per 10 GeV Pi0 mass shift can be explained by simulation
- The difference remains to be better understood

Calibrated 2-Photon Mass

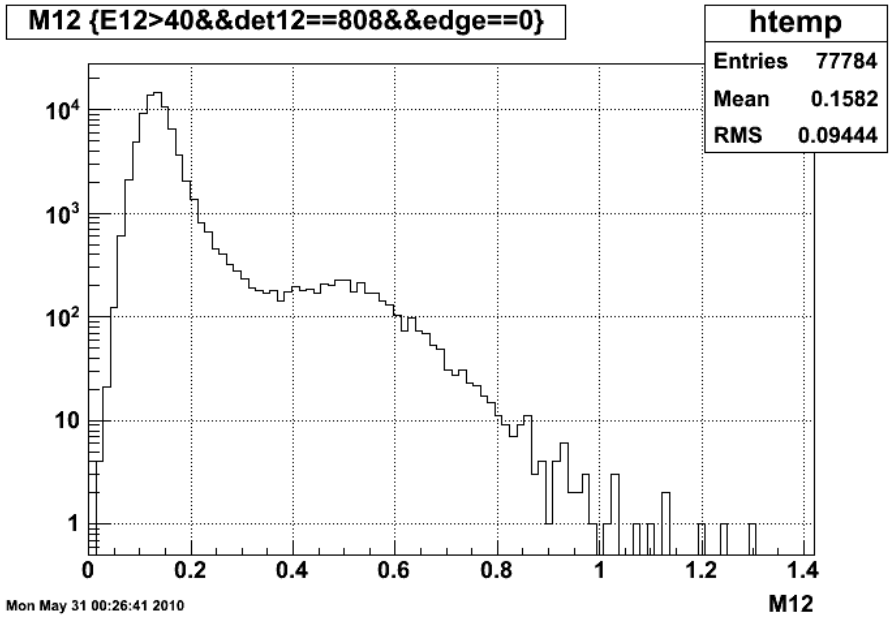

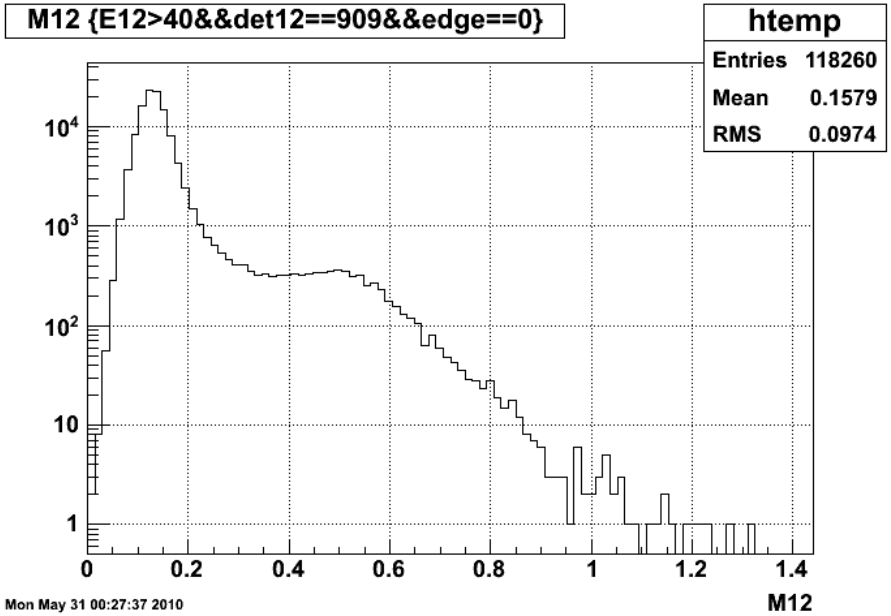

- 2-photon invariant mass distribution for the north-small (left) and south-small (right) detector
- Eta meson peak is clearly seen in the plots

Current Trigger Rate and Pi0 Mass

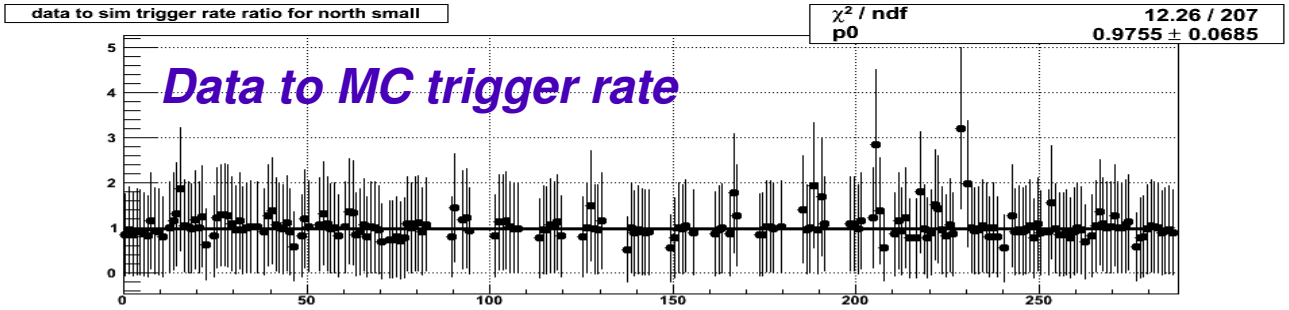

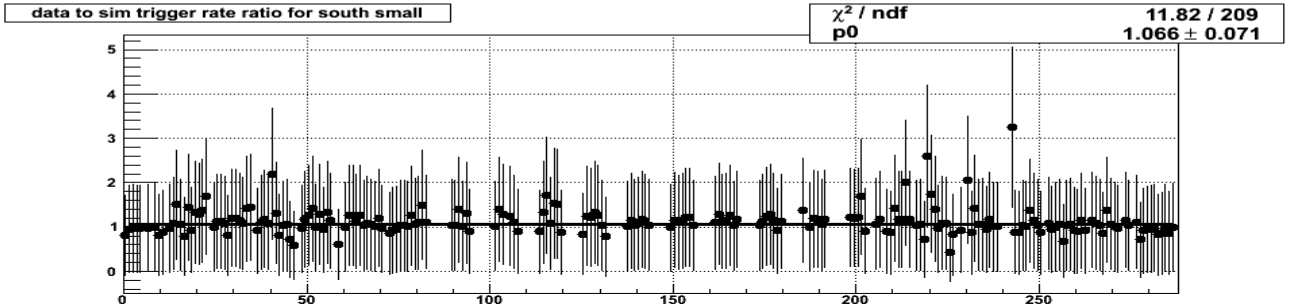

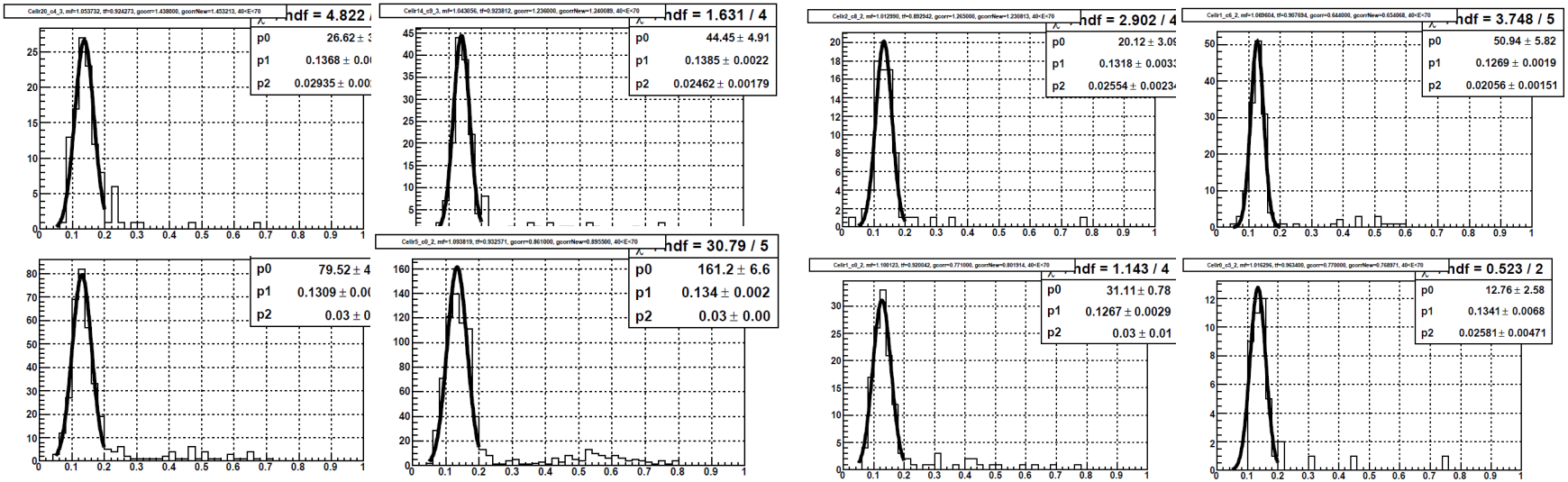

Eta Meson in Run 9 FMS

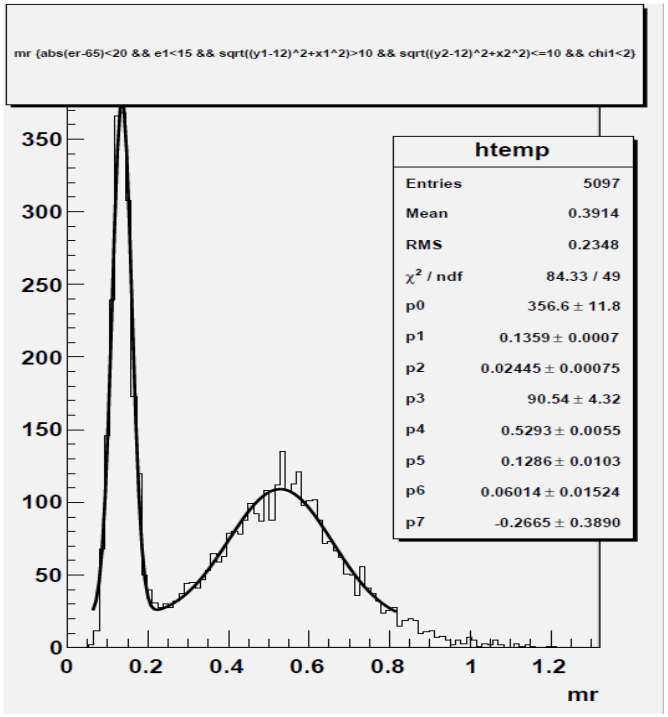

- With better cuts, we can see the eta meson more clearly
- Here we required the high energy photon lies in the inner half region of the detector and the low energy photon lies in the outer half region of the detector

- Preliminary results from a new calibration scheme for the FMS are promising
- Continual work on the calibration and the FMS run 9 data analysis is ongoing
- We will continue to work on the large cells

New Run 9 FMS Calibration

Traditionally, **we've calibrated the forward calorimeters based on on- and off-line π^0 mass peak analysis.** → Worked well for the smaller FPD

With the much larger FMS, (2x49 channels → 1264 channels) the on-line calibration based on π^0 analysis can be too time consuming.

Bigger detector also brings in more features, such as dead cells and edges. It has been known that the π^0 mass analysis can sometimes find local false solutions in the vicinity of dead cells.

For the run 9 off-line calibration, **we are implementing a trigger-rate based calibration method** that compliments the existing π^0 mass analysis.

No reconstruction means the on-line calibration time can be substantially reduced.

It also works better around dead cells and edges, where mass analysis can get confused.

Detailed trigger simulation can be used to set up the FMS trigger for future runs.

Work by Jingguo Ma